Cell Tropism: The Role of Autophagy in Prion Susceptibility

by

Albert Grant Norman

A thesis submitted in partial fulfillment of the requirements for the degree of

Master of Science

Centre for Neuroscience
University of Alberta

ABSTRACT

Prion disease, or transmissible spongiform encephalopathy (TSE), is a type of neurodegenerative disease for which there is no treatment and which is invariably fatal. Prion diseases are distinct in the field of biology and medicine, not only because they can be sporadic, infectious, or inherited, but also because they can transmit disease without the need for nucleic acids. Prion diseases, or prionopathies, arise when PrP^C (the "C" denotes cellular, in relation to the normal version of the protein) which is α-helical rich, misfolds into a pathogenic form (PrP^{Sc} – the "Sc" denotes scrapie, named for the first known prion disease), which is comprised largely of β-sheets, and triggers a cascade of PrP^C misfolding and aggregation, followed by neuronal loss. Prion strains are much different than viral or bacterial strains. Prion strains are defined by their abilities to induce distinct neuropathological deposition patterns of PrP^{Sc}, including distinct areas of involvement within the brain, incubation period, and clinical presentation. While it has been previously established that the disease specific isoform of the prion protein, PrP^{Sc}, is essential for establishing infection, it is not clear how PrP^{Sc} of different strains is able to induce distinct neuropathological profiles. Different cell features may preferentially facilitate strain propagation in certain brain regions; some of these cell features include levels of surface polyanion molecules, levels of PrP^C expression, and membrane lipid content. Another aspect that can vary between cells is the level of basal autophagy, which plays a role in PrP^{Sc} clearance. We hypothesized that basal autophagy can influence cell susceptibility to prions. To investigate the relationship between autophagy and cell susceptibility, we examined the infection efficiency of RML-strain mouse-adapted scrapie prions in three cell lines (N2a, CAD5, and L929) in relation to the cells' basal levels of autophagy. Contrary to our hypothesis, we found that basal autophagy level did not correlate with cell susceptibility in the three cell lines tested. We then modulated

autophagy to determine if we could alter susceptibility to prion infection. Augmentation of

autophagy was able to protect L929 cells from *de novo* prion infection, in addition to clearing

chronically infected CAD5-RML cells of PrP^{Sc} material. We also found that early fluctuations in

autophagy could predict the re-emergence of PrP^{Sc} material in subsequent passages for N2a and

CAD5 cells, but not L929 cells and that an increase in the relative amount of PrP^{Sc} material in

early passages could predict the return of PrP^{Sc} signal in later passages for all three cell lines.

Unfortunately, due to technical issues we were unable to determine if autophagic inhibition

increased cell susceptibility to prion infection. In conclusion, basal autophagy levels did not

correlate with cell susceptibility to prion infection, even though increasing autophagy did reduce

cell susceptibility to prion infection and clear cells of chronic prion infection. Interestingly, early

autophagic flux and levels of PrP^{Sc} predicted whether PrP^{Sc} re-emerged in late passages.

ACKNOWLEDGMENTS

I want to begin by thanking the Neuroscience & Mental Health Institute (formally the Centre for Neuroscience) and the University of Alberta for accepting me into the program, and for giving me the opportunity to study at a well-respected Canadian educational institute.

I want to thank all of my friends and colleagues at the Centre for Prions & Protein Folding Diseases (CPPFD) for all of their advice and moral support, which made work easier and much more enjoyable.

I would also like to thank my committee members Dr. Andrew Simmonds and Dr. Declan Ali for all of their support and guidance throughout my program. Their recommendations unequivalently made my thesis better.

I want to extend my eternal gratification to my supervisors Dr. David Westaway and Dr. Valerie Sim for agreeing to mentor me.

To Dr. David Westaway, I want to thank you for your guidance in my project and in the preparation of this thesis. Without your seemingly limitless knowledge of prions and protein biochemistry you challenged me to elevate the scientific merit of my work, and for that I am a better scientist.

To Dr. Valerie Sim, a simple "thanks" is not nearly enough to describe my appreciation of you as a supervisor. You took a chance on me and accepted me into your lab when others turned me down. You believed in me and helped foster my passion for the prion research. You elevated me when my motivation and mental health waned, and humbled me when I got overconfident. You helped shape me into the researcher I am now.

Finally, to my parents who have supported me financially and emotionally throughout my life there aren't enough words to describe how lucky I am to have you as parents. I can never repay you for what you've done for me, and without your support I am sure I would not be the person I am today.

TABLE OF CONTENTS

TABLES

Table 1: Summary of basal autophagy, basal PrP^C expression, and the effect of autophagic modulation on cell susceptibility to prion infection in L929, CAD5, and N2a cells.

	L929	CAD5	N2a
Basal Autophagy	+++	++	+
Basal PrP^C	+	+++	++
Autophagy Change Under Chronic PrP^{Sc} Infection	N/A	⊘	N/A
De Novo Infection Rate	7/11	0/6	0/6
Trehalose Effect on PrP^{Sc} Infection	0/6	CAD5-RML: 3/3 cleared	N/A
Trehalose Effect on PrP^C	⊘	⊘	↑
Wortmannin Experiment *De Novo* Infection Rate	0/9	4/9	1/6
Wortmannin Effect on PrP^C	↑	⊘	⊘
Early (P2-4) Changes in Autophagy	Negative: ⊘	Negative: ↑ Positive: ⊘	Negative: ⊘ Positive: ↓
Late (P5-7) Changes in Autophagy	Negative: ⊘	Negative: ↑ Positive: ↑	Negative: ↓ Positive: ↓

Table Legend

Symbol	Meaning	Symbol	Meaning
+++	Most	⊘	No Change
++	Mid	N/A	Not Applicable
+	Least	Negative	No PrP^{Sc} return in P6/7
↑	Increase	Positive	PrP^{Sc} return in P6/7
↓	Decrease		

FIGURES
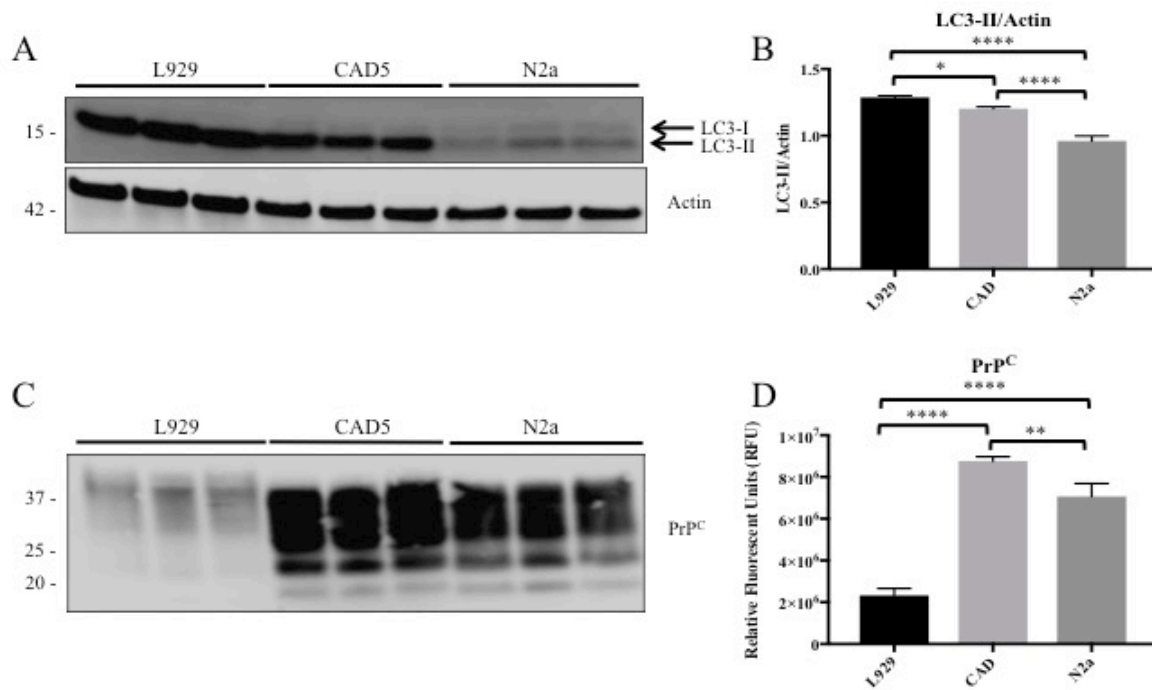
Figure 1: Basal levels of autophagosome formation and PrP^C for L929, CAD5, and N2a cells. (A & C) Immunoblots of LC3-I/II, actin, and PrP^C for L929 (lanes 1-3), CAD5 (lanes 4-6), and N2a (lanes 7-9) cells using an anti-LC3 mAB, anti-β-actin mAB, and anti-PrP mAB (SAF83), respectively (10μg total protein loaded). (B & D) Bar graph representation for L929, CAD5, and N2a cells of (B) endogenous levels of LC3-II in relation to the actin control expressed as a ratio of LC3-II/actin, and (D) PrP^C levels (+/- SD, N=3). Autophagosome formation and PrP^C levels differ significantly between the three cells lines. One-way ANOVA with a post-hoc Tukey's multiple comparisons test for (D & F). *p < 0.05; **p < 0.01; ***p < 0.001; ****P < 0.0001.
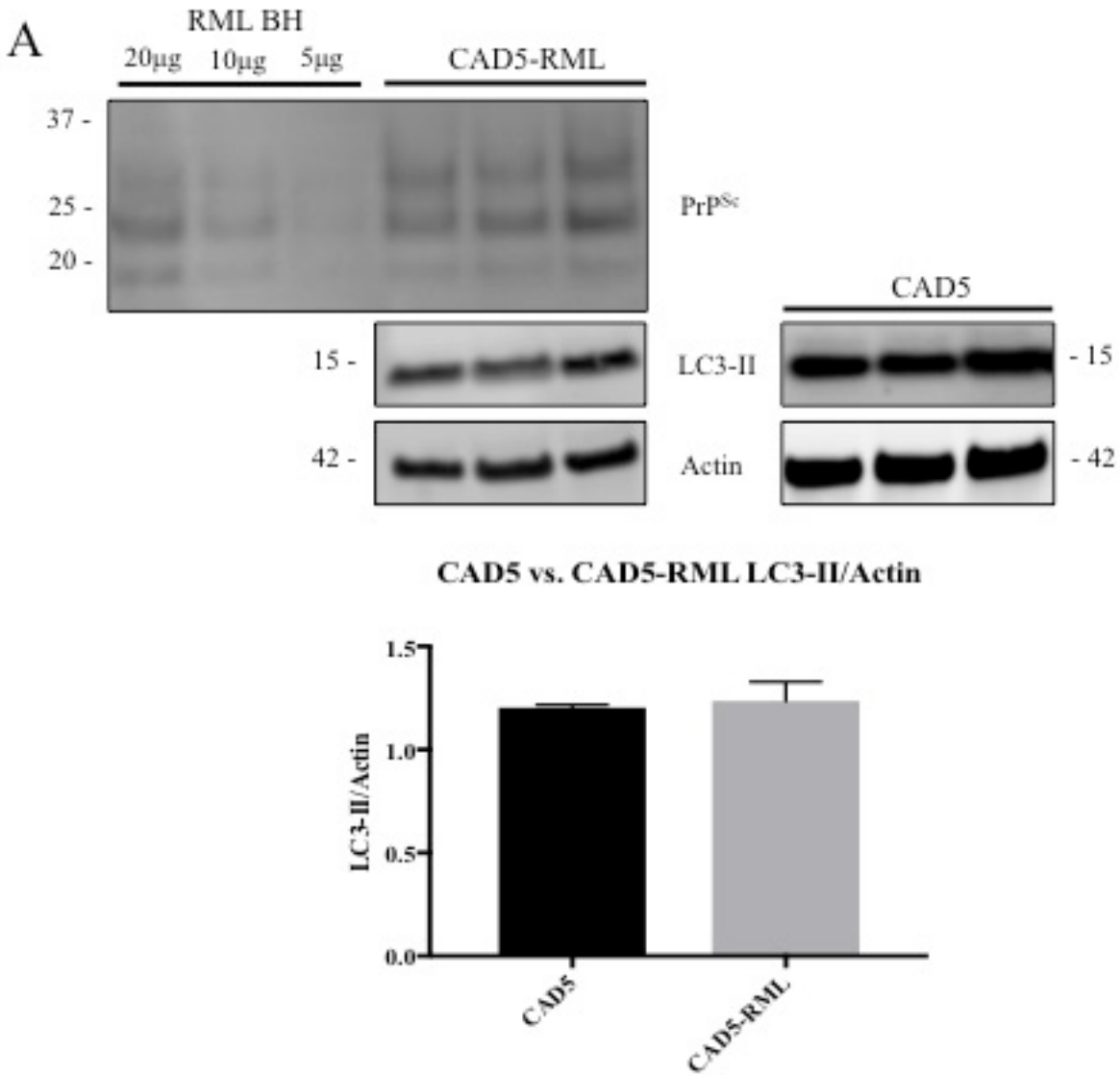
Figure 2: Autophagosome formation and relative PrP^{Sc} levels in the chronically-infected CAD5-RML cell line. (A) Immunoblots of LC3-II and actin for CAD5 (from **Fig. 1**) and CAD5-RML, and PrP^{Sc} levels in CAD-RML cells persistently infected with RML. For LC3 and actin, cell lysates were visualized on an immunoblot using an anti-LC3 mAB or anti-β-actin mAB, respectively (10μg of total protein). For PrP^{Sc}, 30μg of total protein from cell lysates were PK digested and visualized on an immunoblot using an anti-PrP mAB (SAF83). (B) Bar graph representation of endogenous levels of LC3-II in relation to the actin control expressed as a ratio of LC3-II/actin for CAD5 and CAD5-RML cells (+/- SD, N=3).
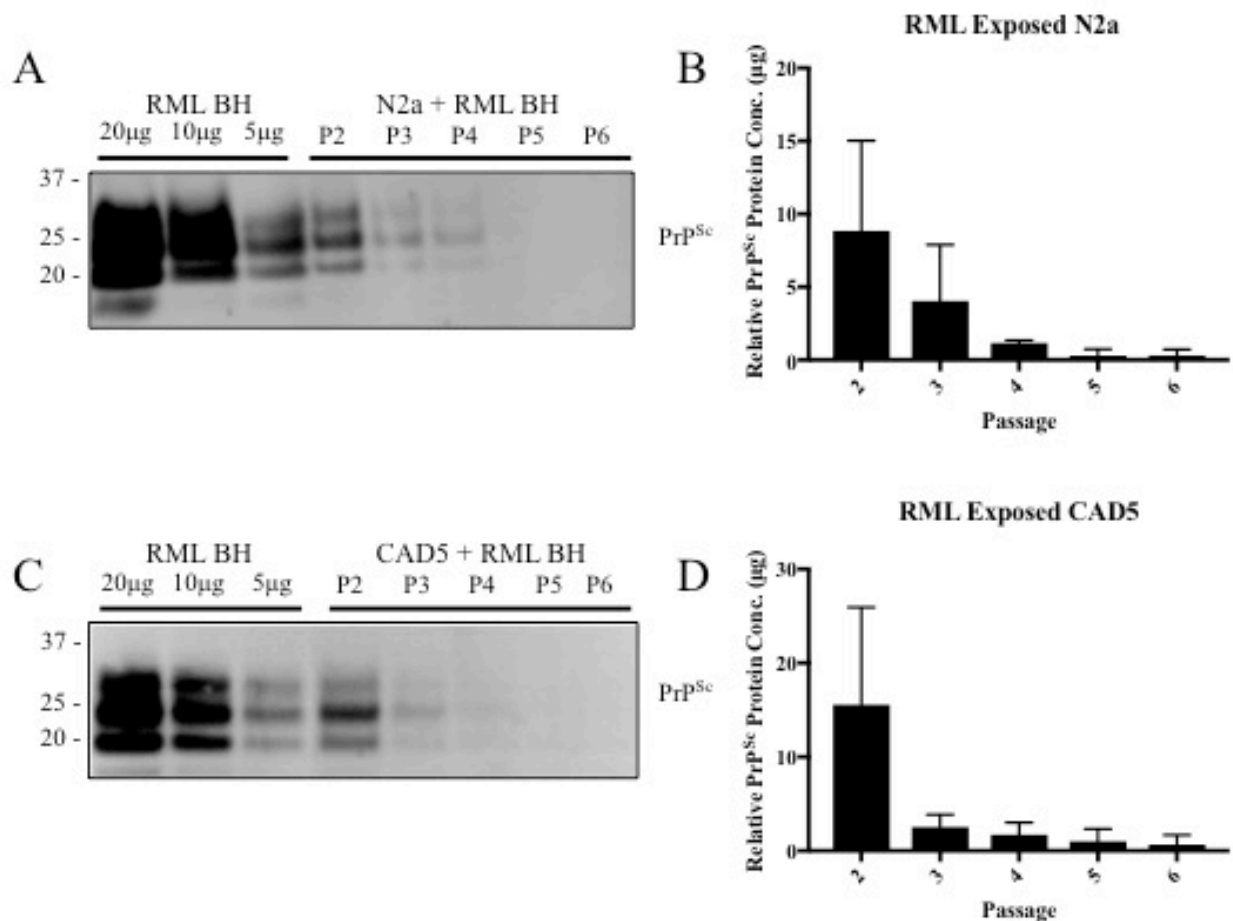
Figure 3: Exposure of RML BH to N2a and CAD5 cells. (A & C) Immunoblots of PrP^{Sc} in (A) N2a and (C) CAD5 cells. Cells were exposed to RML BH at passage 1 and were cultured over the course of six passages (72hrs/passage; P2-6 in lanes 4-8, respectively). 30µg of total protein from N2a cell lysates were digested with PK and PrP^{Sc} levels were visualized by immunoblot using anti-PrP mAB (SAF83). Indicated amounts of protein from an RML BH were PK digested (lanes 1-3) for reference. (B & D) Bar graph representation of (B) N2a and (D) CAD5 cells of the relative amounts of PrP^{Sc} over time in relation to RML BH standards (N2a: +/- SD, N=6; CAD: +/- SD, N=6).

x
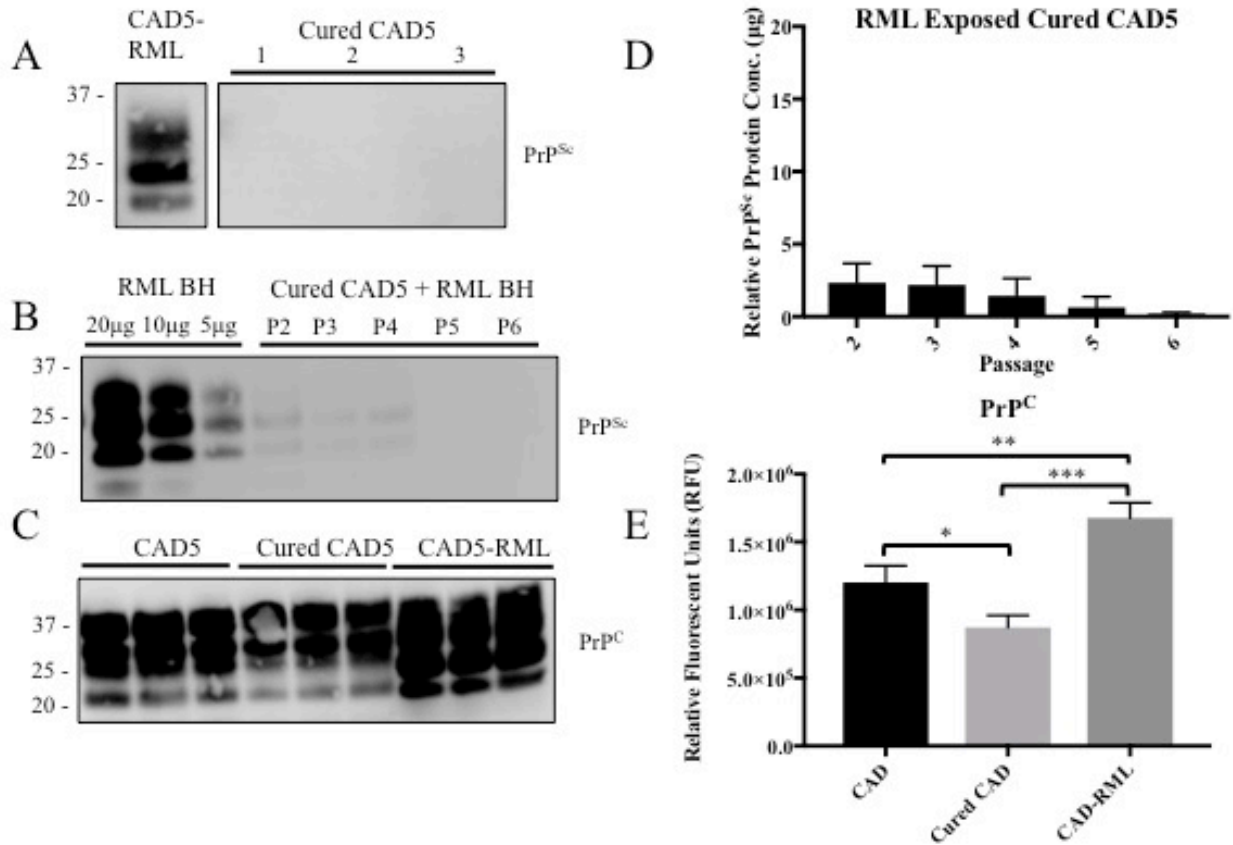
Figure 4: Exposure of RML BH to cured CAD5 cells and relative PrP^C levels before and after curing. (A) Immunoblot of PrP^{Sc} demonstrating curing of CAD5-RML cells. Cells were cured with PPS over 7 passages. 30μg of total protein from cured CAD5 cells were digested with PK and PrP^{Sc} was probed by immunoblot using anti-PrP mAB (SAF83) (N=3). CAD5-RML digested with PK was run on the same blot for comparison. (B) Immunoblot of PrP^{Sc} in cured CAD5 cells. Cells were exposed to RML BH at passage 1 and were cultured over the course of six passages (72hrs/passage; P2-6 in lanes 4-8, respectively). 30μg of total protein from cured CAD5 lysates were digested with PK and PrP^{Sc} levels were visualized by immunoblot using anti-PrP mAB (SAF83). Indicated amounts of protein from an RML BH were PK digested (lanes 1-3) for reference. (C) Immunoblot of PrP^C in CAD5 (lanes 1-3), cured CAD5 (lanes 4-6), and CAD5-RML (lanes 7-9). Undigested cell lysates were probed with anti-PrP mAB (SAF83). (D) Bar graph representation of the relative amounts of PrP^{Sc} over time in relation to RML BH standards (+/- SD, N=6). (E) Bar graph representation of the amount of PrP^C (+/- SD, N=3). Cured CAD cells had significantly less PrP^C than CAD5 and CAD5-RML cells. One-way ANOVA with a post-hoc Tukey's multiple comparisons test. *p < 0.05; **p < 0.01; ***p < 0.001.
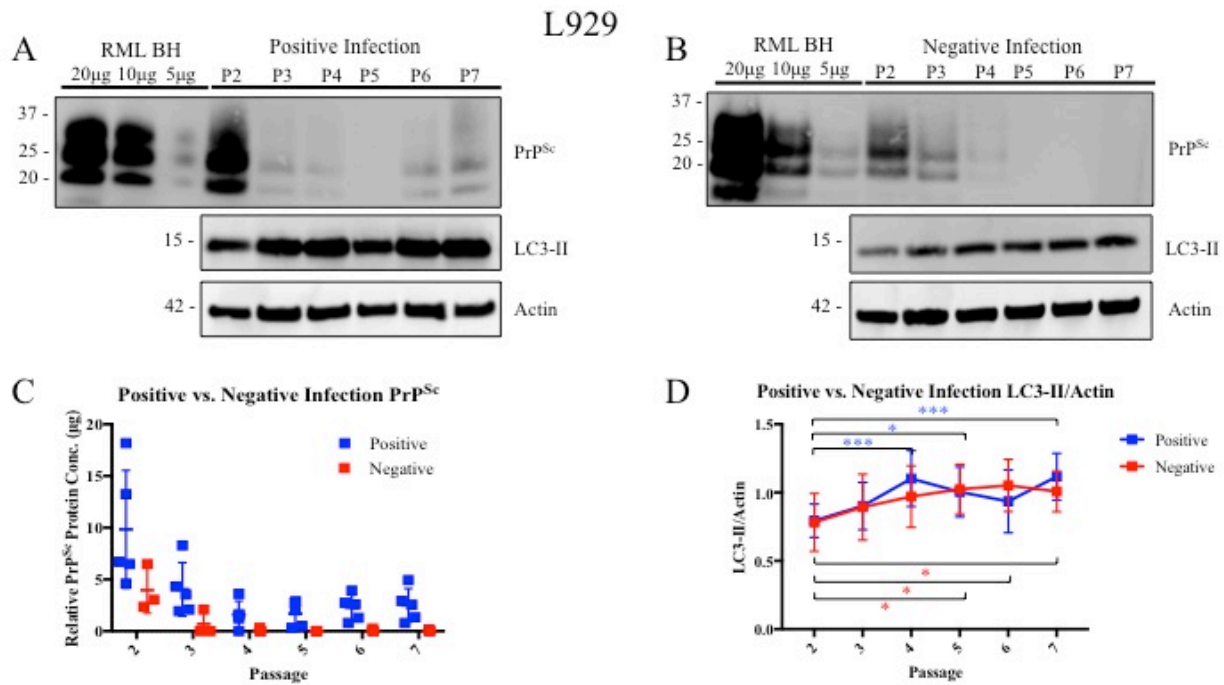
Figure 5: Autophagy after exposure to RML BH in L929 infection experiments. L929 cells were exposed to RML BH at P1 and cultured over the course of seven passages (72hrs/passage; P2-7 in lanes 4-9, respectively). (A & B) Immunoblots of PrP^{Sc}, LC3-II, and actin. (A) In 7 of 11 experiments, PrP^{Sc} was detectable in P6/7; (B) in 4 of 11 experiments, PrP^{Sc} was lost after P4. 30μg of total protein from L929 cell lysates were digested with PK and PrP^{Sc} levels were visualized by immunoblot using anti-PrP mAB (SAF83). Indicated amounts of protein from an RML BH were PK digested (lanes 1-3) for reference. For LC3-II and actin, L929 cell lysates were visualized on an immunoblot using an anti-LC3 mAB or anti-β-actin mAB, respectively (10μg total protein loaded). (C) Bar graph representation for experiments where PrP^{Sc} was detectable in P6/7 (blue, +/- SD, N=7) and where PrP^{Sc} was lost after P4 (red, +/- SD, N=4) of the relative amounts of PrP^{Sc} over the course of seven passages. (D) Bar graph representation of endogenous levels of LC3-II in relation to the actin control in L929 cells where PrP^{Sc} was detectable in P6/7 (blue, +/- SD, N=5) and where PrP^{Sc} was lost after P4 (red, +/- SD, N=3) expressed as a ratio of LC3-II/actin. In experiments where PrP^{Sc} was detectable in P6/7 there was a noticeable decline in autophagosome formation in P5/6, while in experiments where PrP^{Sc} was not detectable in P6/7, autophagosome formation remained elevated. Two-way ANOVA with a post-hoc Sidak's multiple comparisons test for panel (A & B) in relation to P2. *p < 0.05; **p < 0.01; ***p<0.001 (red = negative, blue = positive).
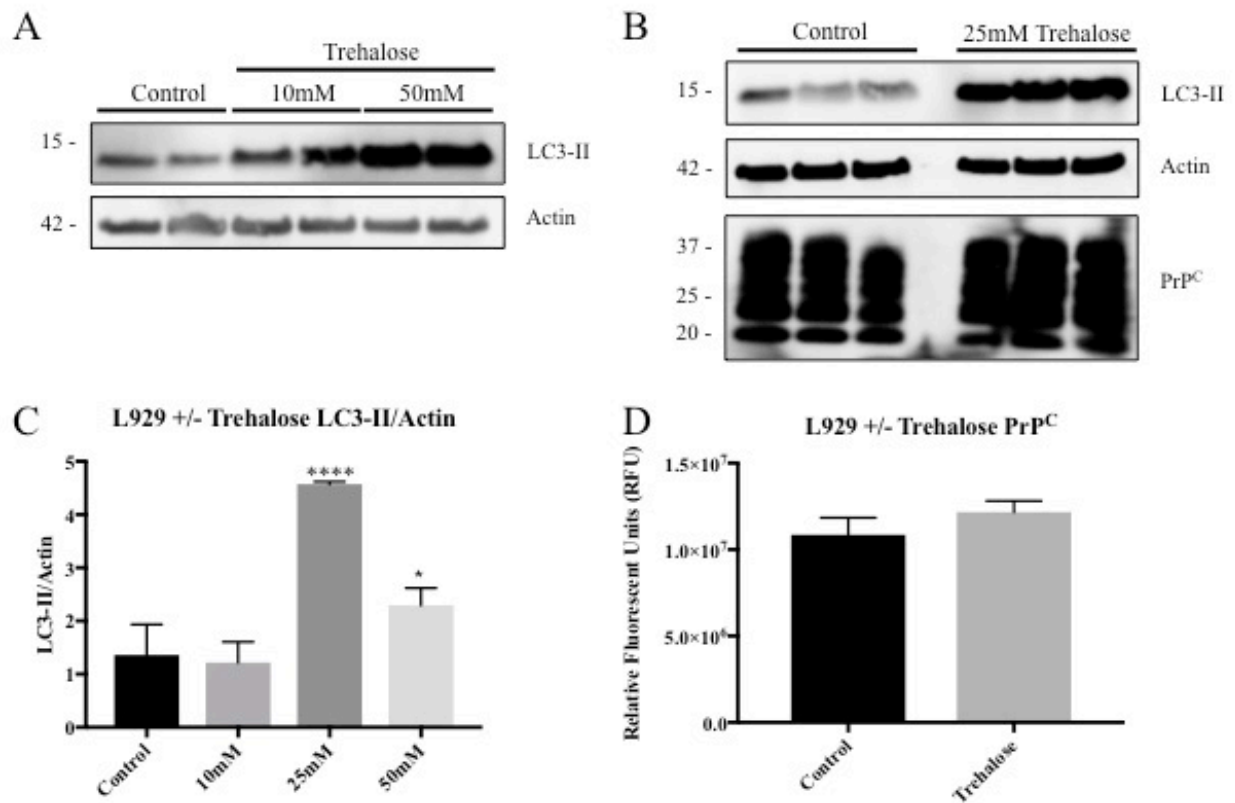
Figure 6: Induction of autophagy in L929 cells by trehalose after 72hrs. (A) L929 cells were either untreated (lane 1 & 2) or treated with either 10mM (lane 3 & 4) or 50mM (lane 5 & 6) trehalose and visualized on an immunoblot using an anti-LC3 mAB (10μg of total protein). (B) L929 cells either untreated (lane 1-3) or treated with 25mM trehalose (lane 4-6) visualized on an immunoblot using an anti-LC3 mAB, including relative PrP^C levels (anti-PrP mAB – SAF83) (10μg total protein loaded). (C) Bar graph representation of the endogenous levels of LC3-II in relation to the actin control expressed as a ratio of LC3-II/actin (+/- SD, Control N=5, 25mM N=3, 10mM & 50mM N=2). (D) Bar graph representation of the amount of PrP^C in L929 cells +/- 25mM trehalose (+/- SD, N=3). 25mM of trehalose induced an increase (~2.5-fold) of endogenous LC3-II. One-way ANOVA with a post-hoc Dunnett's multiple comparisons test for panel (A), unpaired two-tailed t test for panel (C). *$p < 0.05$; **$p < 0.01$; ***$p < 0.001$; ****$p < 0.0001$.
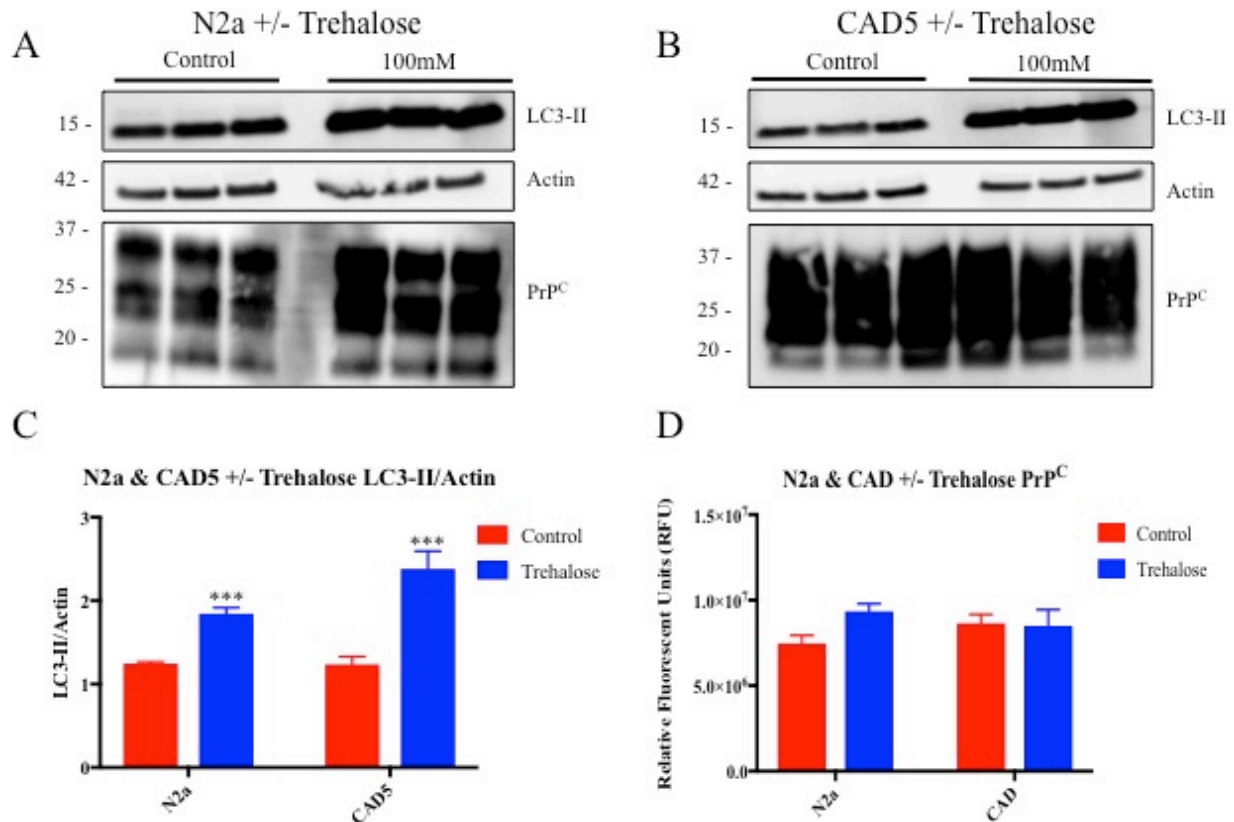
Figure 7: Induction of autophagy in N2a and CAD5 cells by trehalose after 72hrs. (A) N2a and (B) CAD5 cells were either untreated (lane 1-3) or treated with 100mM trehalose (lane 4-6) were visualized on an immunoblot using an anti-LC3 mAB, including relative PrP^C levels (anti-PrP mAB – SAF83) (10μg total protein loaded). (C) Bar graph representation of endogenous levels of LC3-II in relation to the actin control in N2a and CAD5 cells with (blue) and without (red) 100mM trehalose expressed as a ratio of LC3-II/actin (+/- SD, N=3). (D) Bar graph representation of the amount of PrP^C in N2a and CAD5 cells with (blue) or without (red) 100mM trehalose (+/- SD, N=3). 100mM of trehalose induced an increase of endogenous LC3-II in N2a (~1.5-fold) and CAD5 (~2-fold) cells. Notably, there was a significant difference in PrP^C levels in the untreated vs. treated N2a cells, while there was no significant difference for CAD5 cells. Unpaired two-tailed t test for panels (A) and (B). *$p < 0.05$; **$p < 0.01$; ***$p < 0.001$.
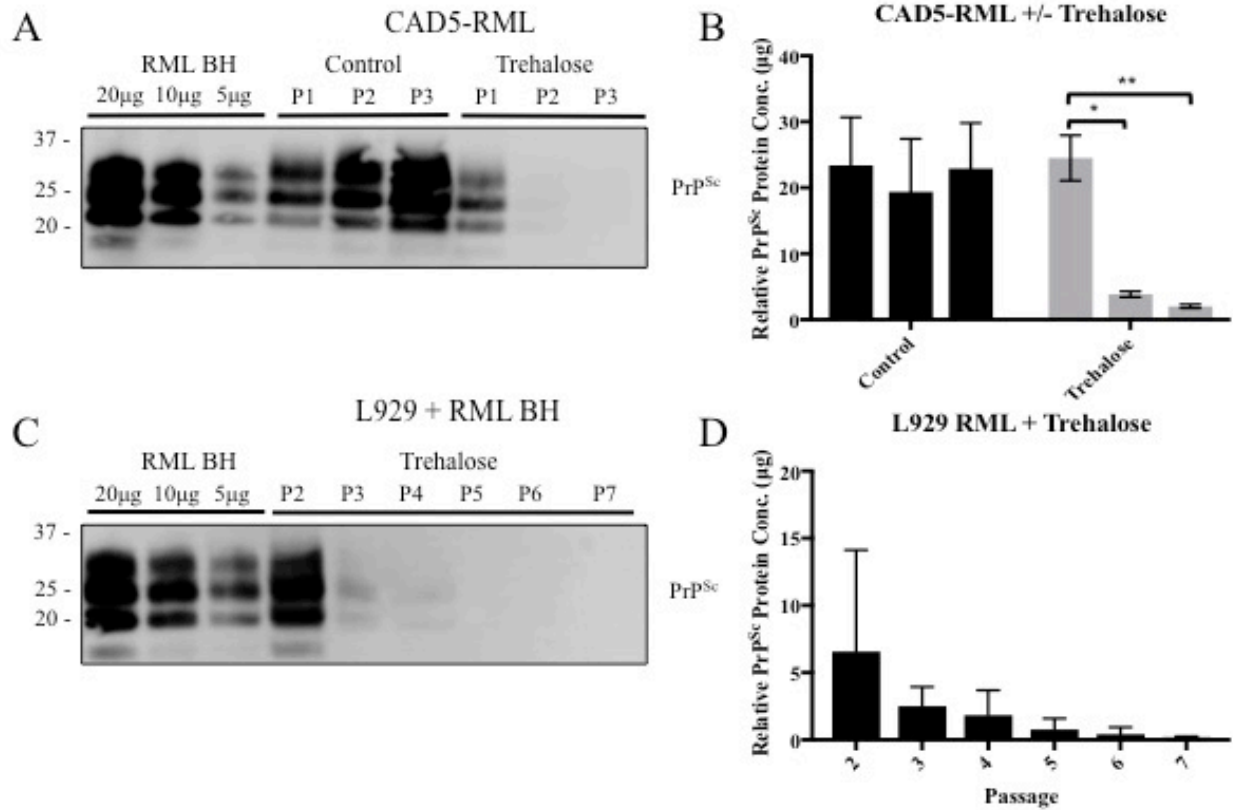
Figure 8: Time-dependent reduction of PrP^{Sc} through induction of autophagy by trehalose.
(A & C) Immunoblots of PrP^{Sc} in (A) chronically infected CAD5-RML cells and (C) L929 cells. Cells were either untreated (P1-3 in lanes 4-6 for CAD) or treated with 100mM of trehalose (P1-3 in lanes 7-9 for CAD5; P2-7 in lanes 4-9 in L929) over three passages (72hrs/passage). 30μg of total protein from cell lysates were digested with PK and PrP^{Sc} levels were visualized by immunoblot using anti-PrP mAB (SAF83). Indicated amounts of protein from an RML BH were PK digested (lanes 1-3) for reference. (B & D) Bar graph representations of the amounts of PrP^{Sc} relative to RML BH standards in (B) CAD5-RML cells over three passages (+/- SD, N=3) and (D) L929 cells over the course of seven passages (+/- SD, N=7). Two-way ANOVA with a post-hoc Sidak's multiple comparisons test for panel (B). *$p < 0.05$; **$p < 0.01$.
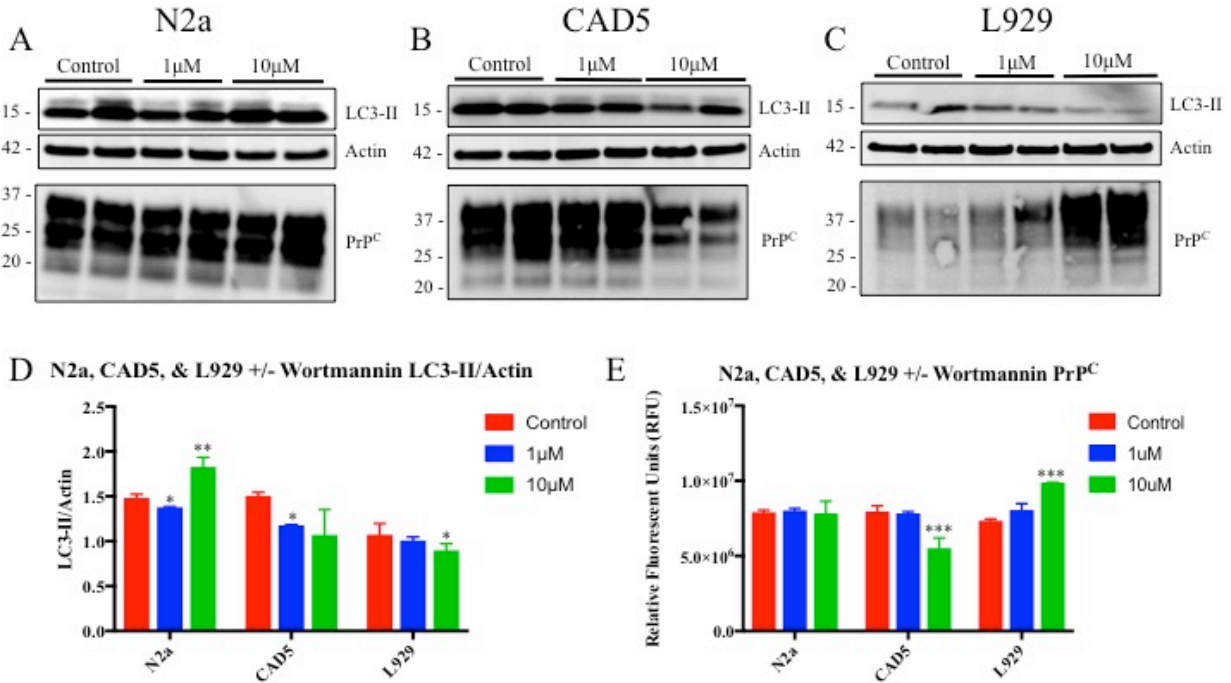
Figure 9: Inhibition of autophagy in N2a, CAD5, and L929 cells with wortmannin after 72hrs. (A-C) Immunoblots of LC3-II, actin, and PrP^C in (A) N2a, (B) CAD5, and (C) L929 cells. Cells were either untreated (lane 1 & 2) or treated with either 1μM (lane 3 & 4) or 10μM (lane 5 & 6) of wortmannin and visualized on an immunoblot using an anti-LC3 mAB and anti-PrP mAB (SAF83) (10μg total protein loaded). (D & E) Bar graph representation for N2a, CAD5, and L929 cells of (D) endogenous levels of LC3-II in relation to the actin control expressed as a ratio of LC3-II/actin, and (E) PrP^C levels after treatment with 1μM (blue) or 10μM (green) in comparison to untreated (red) cells (+/- SD, N=2). One-way ANOVA with a post-hoc Tukey's multiple comparisons test for panels (A-C). *$p < 0.05$; **$p < 0.01$; ***$p < 0.001$.

Figure 10: Autophagosome formation and PrP^{Sc} in N2a cells exposed to RML BH after treatment with wortmannin. N2a cells were exposed to RML BH at P1 and cultured over the course of seven passages (72hrs/passage; P2-7 in lanes 4-9, respectively). (A & B) Immunoblots of PrP^{Sc}, LC3-II, and actin. (A) In 1 of 6 experiments, PrP^{Sc} was detectable in P6/7; (B) in 5 of 6 experiments, PrP^{Sc} was lost after P4. 30μg of total protein from N2a cell lysates were digested with PK and PrP^{Sc} levels were visualized by immunoblot using anti-PrP mAB (SAF83). Indicated amounts of protein from an RML BH were PK digested (lanes 1-3) for reference. For LC3-II and actin, undigested N2a cell lysates were visualized on an immunoblot using an anti-LC3 mAB or anti-β-actin mAB, respectively (10μg total protein loaded). (C) Scatterplot representation for experiments where PrP^{Sc} was detectable in P6/7 (blue, +/- SD, N=1) and where PrP^{Sc} was lost after P5 (red, +/- SD, N=5) of the relative amounts of PrP^{Sc} over the course of seven passages. (D) Mean scatterplot representation of endogenous levels of LC3-II in relation to the actin control in N2a cells where PrP^{Sc} was detectable in P6/7 (blue, +/- SD, N=1) and where PrP^{Sc} was lost after P5 (red, +/- SD, N=5) expressed as a ratio of LC3-II/actin. Two-way ANOVA with a post-hoc Sidak's multiple comparisons test for panel (A & B) in relation to P2. *$p < 0.05$; **$p < 0.01$ (red = negative, blue = positive).
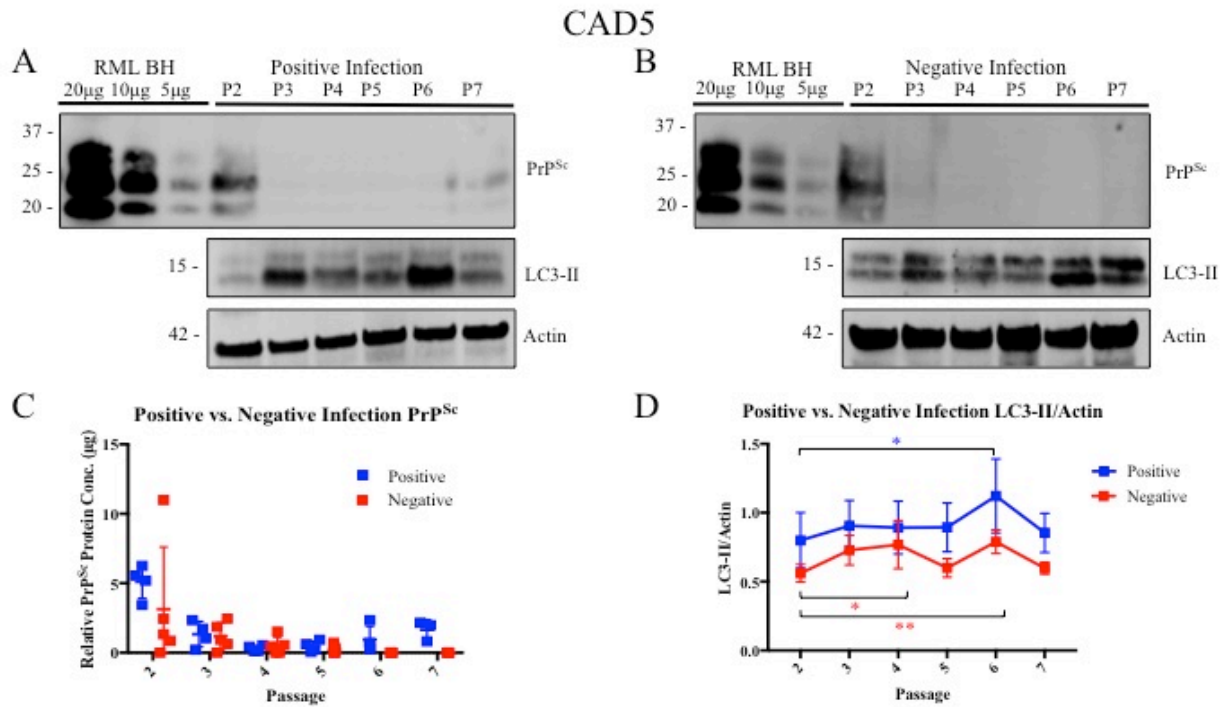
Figure 11: Autophagosome formation and PrP^Sc in CAD5 cells exposed to RML BH after treatment with wortmannin. CAD5 cells were exposed to RML BH at P1 and cultured over the course of seven passages (72hrs/passage; P2-7 in lanes 4-9, respectively). (A & B) Immunoblots of PrP^Sc, LC3-II, and actin. (A) In 4 of 9 experiments, PrP^Sc was detectable in P6/7; (B) in 5 of 9 experiments, PrP^Sc was lost after P4. 30μg of total protein from CAD5 cell lysates were digested with PK and PrP^Sc levels were visualized by immunoblot using anti-PrP mAB (SAF83). Indicated amounts of protein from an RML BH were PK digested (lanes 1-3) for reference. For LC3-II and actin, undigested CAD5 cell lysates were visualized on an immunoblot using an anti-LC3 mAB or anti-β-actin mAB, respectively (10μg total protein loaded). (C) Scatterplot representation for experiments where PrP^Sc was detectable in P6/7 (blue, +/- SD, N=4) and where PrP^Sc was lost after P5 (red, +/- SD, N=5) of the relative amounts of PrP^Sc over the course of seven passages. (D) Mean scatterplot representation of endogenous levels of LC3-II in relation to the actin control in CAD5 cells where PrP^Sc was detectable in P6/7 (blue, +/- SD, N=4) and where PrP^Sc was lost after P5 (red, +/- SD, N=5) expressed as a ratio of LC3-II/actin. Two-way ANOVA with a post-hoc Sidak's multiple comparisons test for panel (A & B) in relation to P2. *$p < 0.05$; **$p < 0.01$ (red = negative, blue = positive).
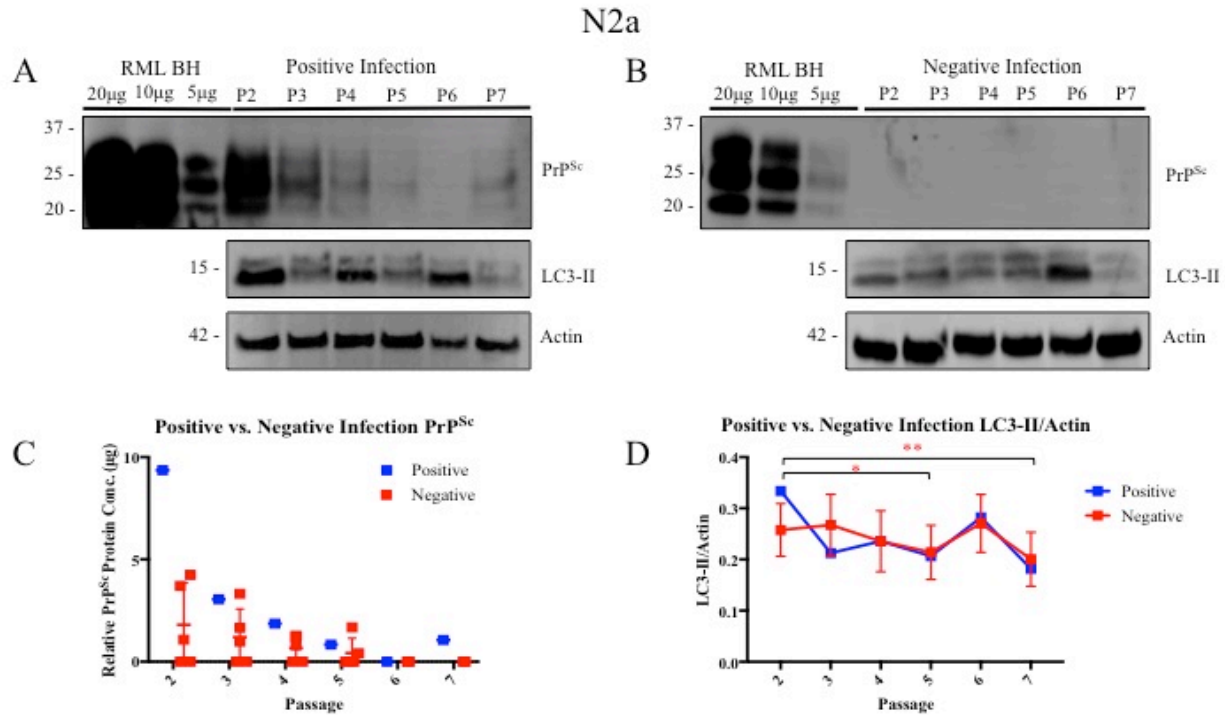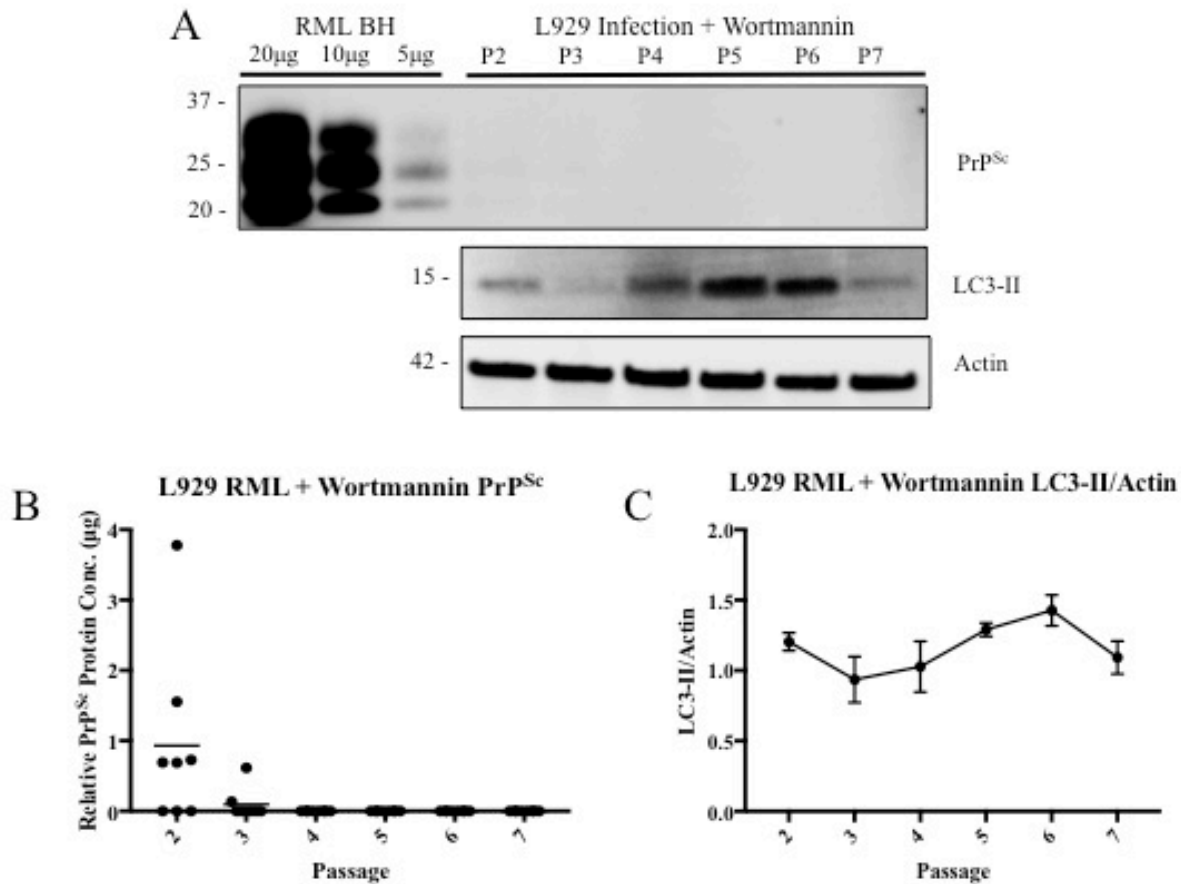
Figure 12: Autophagosome formation and PrP^{Sc} in L929 cells exposed to RML BH after treatment with wortmannin. L929 cells were exposed to RML BH at P1 and cultured over the course of seven passages (72hrs/passage; P2-7 in lanes 4-9, respectively). (A) Immunoblots of PrP^{Sc}, LC3-II, and actin. 30µg of total protein from L929 cell lysates were digested with PK and PrP^{Sc} levels were visualized by immunoblot using anti-PrP mAB (SAF83). Indicated amounts of protein from an RML BH were PK digested (lanes 1-3) for reference. For LC3-II and actin, undigested CAD cell lysates were visualized on an immunoblot using an anti-LC3 mAB or anti-β-actin mAB, respectively (10µg total protein loaded). (B) Scatterplot representation of the relative amounts of PrP^{Sc} over the course of seven passages (N=9). (C) Mean scatterplot representation of endogenous levels of LC3-II in relation to the actin control in L929 cells (+/- SD, N=3).

GLOSSARY OF TERMS

3-MA	3-Methyladenine
22A	22A strain of rodent-adapted scrapie
22C	22C strain of rodent-adapted scrapie
22L	22L strain of rodent-adapted scrapie
87A	87A strain of rodent adapted scrapie
301V	301V strain of rodent-adapted bovine spongiform encephalopathy
AD	Alzheimer's Disease
Ambra1	Autophagy and Beclin Regulator 1
AMPK	AMP-activated protein kinase
AP	Alkaline Phosphatase
APP	Amyloid Precursor Protein
BBB	Blood-Brain Barrier
BCA	Bicinchoninic Acid
Bcl-2	B-cell lymphoma 2
BH	Brain Homogenate
BH3	Bcl-2 homology domain 3
BSE	Bovine Spongiform Encephalopathy
CAD5	Cath-A-Differentiated 5
CJD	Creutzfeldt-Jakob Disease
CNS	Central Nervous System

CO_2	Carbon Dioxide
CWD	Chronic Wasting Disease
DMSO	Dimethyl Sulfoxide
DPBS	Dulbecco's Phosphate-Buffered Saline
dsRNA	Double-Stranded RNA
DY	Drowsy strain of TME
ECM	Extracellular Matrix
EDTA	Ethylenediaminetetraacetic Acid
ER	Endoplasmic Reticulum
ERAD	Endoplasmic Reticulum-Associated Protein Degradation
Fn1	Fibronectin 1
Galt	Galactosyltransferase
GFAP	Glial Fibrillary Acidic Protein
GLUT	Glucose Transporter
GPI	Glycosylphosphatidylinositol
GSS	Gerstmann-Straussler-Scheinker disease
FBS	Fetal Bovine Serum
FFI	Fatal Familial Insomnia
HD	Huntington's Disease
Hsp	Heat shock protein
HY	Hyper strain of TME

Ill 1ra1	Interleukin 11 receptor alpha chain 1
L929	Mouse derived fibroblast cell line
LC3	Microtubule-associated protein light chain 3
LN	Laminin
ME7	ME7 strain of rodent-adapted scrapie
MEM	Modified Essential Medium
mTOR(C)	mammalian Target of Rapamycin (Complex)
N2a	Mouse derived neuroblastoma cell line
N-CAM	Neural Cell Adhesion Molecule
NIH/3T3	Mouse derived fibroblast cell line
NMDA	N-Methyl-D-Aspartate
PCD	Programmed Cell Death
PD	Parkinson's Disease
PE	Phosphatidylethanoamine
PI3K	Phosphoinositide 3-Kinase
PINK	PTEN-Induced Putative Kinase
PK	Proteinase K
PK1	Highly susceptible subclone of the N2a cell line
PPS	Pentosan Polysulfate
Prnp	Prion protein gene
PrP^C	Prion Protein – Cellular; the native form of the prion protein

PrP^{RES}	Prion Protein – Resistant; indicating resistance to Proteinase K digestion
PrP^{Sc}	Prion Protein – Scrapie; the misfolded, disease causing form
PrP^{SEN}	Prion Protein – Sensitive; indicating sensitivity to Proteinase K digestion
PSD-95	Post-Synaptic Density protein 95
PVDF	Polyvinylidene Fluoride
RK13	Prion susceptible cell line derived from rabbit kidney cells
RIPA	Radioimmunoprecipitation Assay
RML	Rocky Mountain Laboratory strain of rodent-adapted scrapie
RNA	Ribonucleic Acid
ROS	Reactive Oxygen Species
SDS	Sodium Dodecyl Sulfate
SLO	Secondary Lymphatic Organs
ssRNA	Single-Stranded RNA
STI1	Stress Inducible protein 1
TBST	Tris-Buffered Saline with Tween 20
TSE	Transmissible Spongiform Encephalopathy
ULK1	Serine/threonine-protein Kinase 1
UPR	Unfolded Protein Response
UPS	Ubiquitin-Proteasome System
VGCC	Voltage-Gated Calcium Channels
WT	Wild Type

Introduction

Prion disease, or transmissible spongiform encephalopathy (TSE), is a type of neurodegenerative disease for which there is no treatment and which is invariably fatal. Prion diseases are distinct in the field of biology and medicine, not only because they can be sporadic, infectious, or inherited, but also because they can transmit disease without the need for nucleic acids [1]. Prion diseases, or prionopathies, arise when PrP^C (the "C" denotes cellular, in relation to the normal version of the protein) misfolds into a pathogenic form (PrP^{Sc} – the "Sc" denotes scrapie, named for the first known prion disease) and triggers a cascade of PrP^C misfolding and aggregation, followed by neuronal loss [2, 3]. Prion disease can affect many mammals including cows as Bovine Spongiform Encephalopathy (BSE) or Mad Cow Disease, cervids as Chronic Wasting Disease, sheep as scrapie, and humans as genetic Creutzfeldt‑Jakob Disease (gCJD, Gerstmann–Sträussler–Scheinker (GSS), Fatal Familial Insomnia (FFI)), sporadic Creutzfeldt‑Jakob Disease (sCJD), or variant Creutzfeldt‑Jakob Disease (vCJD). It has been shown that the presence of PrP^C is necessary for neuropathology to develop, as evident from studies with mice devoid of PrP^C that display resistance to prion disease and show no neuronal loss after inoculation [4].

Structurally, unlike native PrP^C, which contains three α-helices and two β-sheets, PrP^{Sc} has a notable absence of α-helices and is comprised largely of β-sheets [5]. The increase in β-sheet content leads to the formation of amyloid structures that are partially resistant to proteinase K (PK) digestion. On immunoblot, three prominent bands are observed for both PrP^C and PrP^{Sc}, based on different degrees of occupancy of the two N-linked glycosylation sites. After PK digestion, PrP^C is not detectable and the three bands of PrP^{Sc} shift lower on the gel indicating the PK resistant core [6].

The Function & Interactome of the Prion Protein

The normal physiological function of PrP^C is unclear. At present, there are many different functions attributed to PrP^C, including regulation of the immune system, copper binding and synaptic transmission, signal transduction, anti-apoptotic functions, as well as cell adhesion [7]. With these various proposed functions, there are a number of interactions of PrP^C with other proteins/ligands through which PrP^C can exert its effects [8-12]. In the immune system, PrP^C is

1

widely expressed on haematopoietic stem cells and mature lymphoid cells and is upregulated upon T cell activation, however its role in T cell function is still not clear [13]. PrP[C] has also been shown to colocalize with the major histocompatibility complex class II (MHC class II) in monocyte-derived dendritic cells [13]. The synapse, PrP[C] is present in both pre- and post-synaptic structures, which would indicate plays a role in neuronal communication [14, 15]. Additionally, when nerve endings are depolarized they release copper into the synaptic cleft [16], and since PrP[C] is known to be able to bind copper [17], this further supports a functional role for PrP[C] in the synapse. It is possible that presynaptic PrP[C] could buffer copper levels in the synaptic cleft, which would protect synapses from reactive oxygen species (ROS) generated via redox reactions. Due to the concentration of copper in the synaptic cleft, PrP[C] may also play a role in calcium homeostasis through modulation of voltage-gated calcium channels (VGCC) [18, 19]. This ROS scavenging ability contributes to its anti-apoptotic nature, as increases in intracellular ROS levels have been linked to apoptosis [20]. PrP[C] has also been shown to play a role in cell adhesion. Experiments where formaldehyde was used to cross-link PrP[C] with other proteins showed that the N-terminal portion along with the first helix interacted with neural cell adhesion molecules (N-CAMs) [21].

PrP[C] has also been implicated in behaviour and memory. In *Prnp*[0/0] mice with the null allele designated ZrchI, elimination of PrP[C] leads to an increase in locomotion when exploring novel environments [11]. These mice also showed an increased response to an antagonist of the NMDA receptor, MK-801, but normal responses to amphetamines and caffeine when compared to wild-type mice (WT) [22]. This may be due to the role PrP[C] plays in synaptic modulation, where it has been shown to interact with post-synaptic density 95 (PSD-95), inhibiting N-methyl-D-aspartate (NMDA) receptors through which PSD-95 interacts [23, 24]. With respect to memory, there are at least two molecular interactions that can mediate the effects of PrP[C] on memory consolidation/retention, namely hop/stress inducible protein 1 (STI1) and laminin (LN) [25, 26]. Most interestingly, PrP[C] has interactions with proteins that have been implicated in other protein misfolding diseases, namely Alzheimer's disease (AD) [27, 28]. Studies have shown that PrP[C] expression inhibits the cleavage of the amyloid precursor protein (APP) by the enzyme β-secretase, thereby reducing the formation of β-amyloid which is a major contributor to senile plaques [29].

Life Cycle of the Prion Protein

The human *Prnp* gene is located on the short arm of chromosome 20, contains two exons, and is highly conserved throughout mammals [30, 31]. The primary sequence for the prion protein is 253 amino acids (in human, 254 in mice) and is post-translationally modified with amino- and carboxy- terminal signal peptides that aid it its transport to the cell surface [32]. A glycosylphosphatidylinositol (GPI) anchor attached to the carboxy terminus serves to anchor the protein to the cell membrane [33]. PrP^C is widely expressed throughout the nervous system, although its ubiquity can vary among cell types and brain regions [11, 34].

When PrP^C misfolds into PrP^{Sc}, either through spontaneous conversion or interaction with other misfolded PrP^{Sc} (acquired), it needs to be internalized via the endosome system and broken down to prevent further PrP^C conversion. There are two main avenues that PrP^{Sc} can follow in order to be broken down, namely the ubiquitin-proteasome system (UPS) and the lysosomal/autophagic pathway. The UPS is one of the major cellular protectors against misfolded proteins in mammals. In this system, misfolded prions are marked for proteasomal degradation by tagging with ubiquitin in a reaction that involves three main enzymes: ubiquitin activating enzymes (E1), ubiquitin conjugating enzymes (E2), and ubiquitin ligases (E3) [35, 36]. Once a protein is tagged, the multi-subunit barrel-shaped complex known as the proteasome can break it down [37]. When the UPS is impaired, autophagy (discussed later in the context of prion disease) is usually upregulated to facilitate the breakdown of the larger aggregates.

When both mechanisms fail to rid the cell of PrP^{Sc}, the proliferation of PrP^{Sc} overwhelms the cell and will eventually lead to neurodegeneration.

Outside of spontaneous conversion of the prion protein, prion disease can be acquired. Prions are able to enter and infect host organisms via multiple routes including, but not limited to, the enteric system, the circulatory system, and the nervous system, however the replication of PrP^{Sc} can vary by strain. In the enteric system, prions are able to enter through the Peyer's patches via exploitation of the enterocyte M-cells (Microfold cells), which continuously sample the intestinal lumen as a means of immunosurveillance [38]. After crossing the follicle-associated epithelium (FAE), prions spread. Some prion strains can also be efficiently transmitted through the blood or blood derivatives, as demonstrated in sheep that were infected with BSE and scrapie

via whole-blood transfusions [39] . Before invasion of the CNS, prions from diseases such as CWD, transmissible mink encephalopathy (TME), and natural scrapie tend to accumulate and replicate within secondary lymphoid organs (SLO); these diseases are designated as "lymphotropic" prion diseases [40, 41] . Other prion diseases, such as CJD or classical BSE, directly invade the CNS without having to be replicated peripherally [42] . These prion diseases are referred to as "neurotropic" [42] .

Prion Strains

Prion strains are defined much differently than those of viruses or bacteria. Bacterial or viral strains are genetic variants based on changes to their encapsulated genomic nucleic acids. Prion strains, on the other hand, are not solely defined by genetic means. Prion strains are prion isolates that, upon inoculation into genetically identical hosts, cause prion disease with consistently distinguishable characteristics [43] . These characteristics include incubation time, biochemical properties (western blot banding profiles and heat/chemical denaturing profiles), as well as pathological profile [44, 45] .

Strains can occur within prion proteins of the same amino acid sequence. This is evident from studies showing how transmission of one particular prion strain (scrapie) can be transmitted to the same genetically identical host (C57/BL6 mice) and produce distinct disease phenotypes. These features remain even after serial passage within the same species [46] . For example, there is a wide range of verifiably different (rodent-adapted) scrapie strains that can arise in the same genetic host, such as RML, 22L, ME7, 22C, 87A, and 22A, among others [44] . This suggests that even with identical primary structures, the prion protein can misfold into different conformers, possibly with the aid of other cellular co-factors [47, 48] .

The main parameter that allows for different prion strains to arise is the conformational structure that the prion protein adopts. This 3D structure can be influenced by polymorphisms in the *Prnp* gene. These polymorphisms can result in drastically different prion diseases or differences in susceptibility to prion disease. For example, in humans there is a polymorphism at codon 129, which can be either a methionine or a valine, resulting in three possibilities: MM, MV, or VV. Homo- or heterozygosity at this position determines not only susceptibility to prion disease, with MV heterozygosity being less susceptible to prion disease than MM or VV

homozygosity [49] , but it can also influence which prion disease arises in the presence of disease-causing mutations within *Prnp*, such as codon 178. The normal amino acid at codon 178 is an aspartic acid (D). If this codon is mutated to asparagine (N) in *cis* with methionine at codon 129, the resulting disease is fatal familial insomnia (FFI) [50] . However, if the codon at 129 is a valine, the disease is familial CJD [50] . Other mutations that can cause prion disease include, but are not limited to, E200K (gCJD) and P102L (GSS) [51] . In addition to mutations that cause disease, recently the mutation G127V has been found which confers resistance to prion disease [52] .

The Species Barrier & Prion Cell Tropism

Prion isolates from one species tend to be less infectious to other species, as evident by longer incubation times or the absence of the disease in these other species. This is referred to as the "species barrier" [53, 54] . This barrier is thought to be due to differences between the inoculum and the host prion protein sequence. For any given PrP sequence, there may be a preferred range of conformations that it can adopt. Depending on the conformation of PrP^{Sc} to which a given PrP sequence is exposed, it may not readily be converted. The species barrier can be so strong that certain hosts do not develop clinically defined prion disease in their lifetimes. It has been proposed that the main driving force behind the relative difficulty of prion transmission is the overlap, or lack of overlap, of permissible PrP^{Sc} conformations between PrP primary structures from the two species [54] . This scenario is known as the "cloud hypothesis," which stipulates that in a given inoculum, there may be many different conformations of PrP^{Sc} and that one particular isoform may be favoured in one host, while another isoform may be favoured in a different host [54] . This hypothesis can help explain how after serial passages in the same host, incubation periods tend to shorten. This trend is referred to as "strain adaptation." Evidence strongly supports the hypothesis that the main factor in strain diversity is the structural conformation of PrP^{Sc} [55, 56] , but the mechanism responsible for strain-specific differences in neuropathology is still unknown.

The presence or absence of PrP^{C} is not the sole factor that will determine prion susceptibility. Certain cellular cofactors, such as polyanions and lipids, have been implicated in prion conversion, although the precise mechanism remains unclear [48] . Although both lipids and polyanions have an effect on prion propagation, polyanions do not seem to be necessary for prion infectivity [57] . In contrast, lipids not only influence propagation, they also have a significant

effect on prion infectivity, with purified prions re-incorporated into liposomes showing almost a hundred-fold increase in infectivity [58]. Additionally, cellular regulatory mechanisms, such as autophagy (covered in the following sections), can also have an effect on a cells susceptibility to prion infection.

Prion diseases are associated with a set of histopathological features: spongiform vacuolation, neuronal loss, astrocytosis, and PrP^{Sc} deposition [59]. Vacuolation occurs within the cell body and neuronal processes, and can be found in various areas of the brain, depending on the prion strain in question [60-62]. In the rodent-adapted scrapie strains 139A, ME7, and 22L, differences in incubation periods and vacuolation were observed in wild-type mice after inoculations in different brain regions (cerebral cortex, caudate nucleus, thalamus, substantia nigra, and cerebellum) [63]. ME7 and 139A showed the same pattern of vacuolation regardless of the inoculation site, whereas 22L showed similar patterns in vacuolation in the cerebral cortex and thalamus, but showed more lesions in the cerebellum with little to no vacuolation in other areas [63]. Neuronal loss can be variable in severity and distribution, and tends to be the most severe in cases with prolonged clinical history [59]. Astrocytosis is also variable, but is sometimes the most prominent feature [64]. Astrocytosis generally parallels vacuolation and neuronal loss [65]. In addition to these features, PrP^{Sc} accumulates in the neuropil as diffuse plaques, but can occasionally be found in the soma of neurons [65]. This PrP^{Sc} deposition, which can be in the form of amyloid plaques, can present variably based on the prion strain [55].

Strain-specific differences in neuropathology can be attributed, in part, to the specific cell that is affected, as not all cell types are susceptible to prion infection. This is referred to as a prion strain's *cell tropism*. The standard scrapie cell assay (SSCA) is designed to measure infectivity in different cell types and can demonstrate cell tropism, as certain cell lines are easily infectable, while others are not. RML and 22L are common prion strains used in the SSCA to determine infectivity, and have been shown to infect neuronal cells lines (N2a – mouse neuroblastoma, CAD5 – mouse catecholaminergic cells) and non-neuronal cell lines (C2C12 – mouse myotube, RK13 – rabbit kidney epithelial cells, L929 – mouse fibroblasts) [66]. Most cell lines, in general, are not permissive to prion infection or replication, and even those lines that are infectable may not necessarily be permissive to all strains [66]. For example, even though the N2a-derived PK1 cells are susceptible to RML and 22L, they are resistant to ME7, 22A, and 301V [67].

There are also chemical agents that can alter the composition of the prion "cloud", allowing for certain isoforms of a given strain to be selected for that are more infectious. For example, Weissmann and colleagues used the chemotherapeutic drug swainsonine to artificially select for resistant prion substrains in PK1 cells [68, 69]. Swainsonine (swa), which potently inhibits the Golgi α-mannosidase II enzyme (involved in the processing of N-linked glycans), was shown to protect against RML infection while also inhibiting the replication of certain 22L prion substrains (swa-sensitive - ~99% of the prion population) while remaining ineffective against other 22L prion substrains (swa-resistant - ~0.5% of the prion population), thereby selecting for a particular subtype of prions [68].

The basis for why certain cell types are susceptible to certain prion strains while resistant to others is not fully understood, but it can be attributed, in part, to a given cells regulatory functions and its interaction(s) with other cellular proteins.

Cell Death

Cell death is a prominent feature in neurodegenerative diseases. Based on morphology classification by Schweichel & Merker, there are three types of programmed cell death (PCD) that can be discriminated: apoptosis (Type I), autophagy (Type II), and cytoplasmic cell death (Type III) [70]. Apoptosis is characterized by chromatin condensation, cell shrinkage, plasma membrane blebbing, and fragmentation of the nucleus [20]. Morphologically, macroautophagy (hereafter referred to as autophagy) is characterized by autophagic vacuoles in the cytoplasm (double membrane structures used to house cargo destined for degradation), mitochondrial permeabilization, and enlargement of both the Golgi and endoplasmic reticulum (ER) [71]. Cytoplasmic cell death is similar to autophagy with the notable absence of lysosomal involvement, but is also characterized by swelling of sub-cellular organelles, leading to the formation of large empty spaces within the cytoplasm which fuse to the extracellular space, resulting finally in the disintegration of the cellular structures [71, 72]. Type III cell death is now more commonly referred to as necrosis [20]. Since the characterization of these main PCD types, many other types of specialized cell death have been described [73].

In addition to all the other cellular effects PrP^C has, it also has a role(s) with respect to cell death. Evidence supports PrP^C having functions that are anti-apoptotic, as it has been shown

to directly inhibit Bax-induced apoptosis [74, 75] and can also act, in tandem with other known signaling proteins such as B-cell lymphoma 2 (Bcl-2), as a cellular receptor for neuroprotective signals [75-77]. PrP^{Sc} is only toxic when neurons express GPI-anchored PrP^C, as studies in which only other cell types expressing PrP^C (oligodendrocytes) while neurons were devoid of PrP^C showed intrinsic resistance to prion infection [78]. Additionally, it seems as though the GPI anchor plays a role in disease formation, as Chesebro and colleagues showed that scrapie infection of mice devoid of the GPI anchor resulted in an infectious amyloid-based disease without the clinical signs of scrapie [79]. There is, however, no conclusive evidence when it comes to whether neurons die of apoptosis in prion disease. Some labs find no evidence of apoptotic cell death in their studies of prion disease [80-82] while others readily find it [72, 83]. Autophagy is a highly conserved regulated process that cells use to rid themselves of misfolded proteins and other unwanted/unneeded cellular constituents. Since neurodegenerative diseases such as AD, PD, HD, and prion disease share a core component in pathology, namely the misfolding of a normal cellular protein, studying the role autophagy plays in these diseases is extremely important. Thus, research into the role autophagy plays in relation to prion pathogenesis has been a hot topic of study as of late [75, 84-86].

Studies have shown autophagic vesicles in neurons in other protein misfolding diseases such as Alzheimer's, Parkinson's, and Huntington's, all of which have been proposed as "prion" diseases [87]. In the context of prion disease, it has been shown that increasing autophagy can be beneficial in both cell and animal models [87, 88]. Autophagy is classically induced through starvation (as above), but can also be chemically induced with agents that work both in mammalian target of rapamycin (mTOR) dependent and independent manners [89, 90]. Interestingly, Ishibashi and colleagues used multiple prion strains (Chandler, 22L, Fukuoka-1) in one cell type (N2a) to show that modulating autophagy has varying results in clearance and associated PrP^{Sc} levels among different prion strains. The interesting caveat to this work is that the researchers only went forward and studied autophagic modulation in the N2a cells infected with Fukuoka-1, as the other two strains (Chandler & 22L) did not show much, if any, response to autophagic modulation [90].

<u>Hypothesis</u>

In prion diseases it has been shown that different strains present with different pathology in the brain. This difference in pathology is likely due to some characteristic of the cells in a given brain region, where certain cells are naturally more susceptible to certain prion strains than others. One of the features that all cells possess is the ability to undergo autophagy, and since it is clear that autophagy plays a role in most protein-misfolding diseases, including prion diseases, it is possible that the autophagic flux of a given cell is one of the factors that governs which areas of the brain will be affected by a given prion strain.

With respect to the above, this study set out to answer two main questions:

1. Does a cell's basal level of autophagy influence its susceptibility to prion infection?

2. Can variation in basal autophagy amongst cell types explain the different neuropathological profiles elicited by different prion strains?

We postulate that basal autophagy is a determinant of prion infectibility. Given this, we predict that cell susceptibility, as defined by the ability of a given cell type/line to develop a consistent prion infection, correlates with basal autophagy. In addition, we predict that augmentation of autophagy will decrease cell susceptibility and inhibition of autophagy will increase cell susceptibility.

Methods

Reagents

D-(+)-Trehalose was purchased from Fisher Scientific (Cat: BP2687-100). Wortmannin was also purchased from Fisher Scientific (Cat: W1628-1MG) and was dissolved in DMSO (Fisher Scientific Cat: BP321-1) at a stock solution of 2mM and stored at -20°C. Pefabloc proteinase inhibitor (Cat: 11429868001) and proteinase K (Cat: 25530-015) were both purchased through Fisher Scientific. Anti-PrP mouse monoclonal antibody (SAF83) was purchased from Bertin Pharm (Cat: A03207). Anti-LC3 polyclonal antibody was purchased from MBL (Cat: PM036). Anti-β-actin mouse monoclonal antibody was purchased through Sigma Aldrich (Cat: A5441). Cell culture media was obtained through Fisher Scientific.

Cell Culture

The mouse fibroblast cell line L929 (American Tissue Culture Collection CCL-1) was maintained in Modified Essential Medium (MEM – with Earl's salts, L-glutamine, and sodium bicarbonate) containing 10% heat inactivated fetal bovine serum (HI-FBS – Fisher Scientific Cat: 16140071) and 1% v/v of a stock solution of penicillin (10000units/mL)/streptomycin (10000μg/mL) (Fisher Scientific Cat: 15140-122) in a 5% CO_2 atmosphere. The mouse neuroblastoma cell line N2a (American Tissue Culture Collection CCL-131) and the mouse catecholaminergic neuronal tumour cell line CAD5 (Cath.-a-differentiated)/CAD5-RML (a generous gift courtesy of Dr. Hermann Schätzl from the Hotchkiss Brain Institute, University of Calgary) were both maintained in Opti-MEM (+ HEPES, 2.6g/L sodium bicarbonate, and L-glutamine) containing 10% FBS and 1% v/v penicillin/streptomycin stock in a 5% CO_2 atmosphere. All cell lines were maintained in a 75cm^2 flask (Fisher Scientific Cat: 12556010) and were split (1:4) and passed when confluency was 85-95% (approx. every 3-4 days).

De Novo Infections & Drug Treatment

De novo infections were performed by adding 30μL of a 10% (w/v) Rocky Mountain Laboratory (RML) strain of mouse-adapted scrapie brain homogenate (BH) to 300μL of cells and 700μL of cell culture media. After 15 minutes, another 1mL of culture media was added and cells were cultured for 3-4 days per passage. Confluent cells were washed twice in Dulbecco's

Phosphate Buffered Solution (DPBS – Fisher Scientific Cat: 14190-144) and resuspended in 2mL of DPBS. From this, 500μL of the resuspended cells were passed into 2mL of fresh media and the remaining 1.5mL was collected for analysis. Infectious BH was only used for the first passage and then normal media was supplemented for the remaining passages. Cells were cured of PrP^{Sc} material using pentosan polysulfate (PPS – gift from Dr. Debbie McKenzie, University of Alberta) at a concentration of 10μg/mL, supplemented in the media during each passage for seven (7) passages. Curing of cells was verified by digestion of samples with proteinase K (PK) and subsequent analysis by immunoblot for the presence of PrP^{Sc} material.

Drug treatment of all the cell lines was performed in Corning 6-well sterile plates (Fisher Scientific Cat: 07-200-83) by adding 25mM (L929) or 100mM (CAD5-RML) of D-(+)-trehalose to the culture media for the duration of the passage (72hrs). Wortmannin was diluted from the stock concentration (above) and added to the culture media at final concentrations of 1μM or 10μM for N2a/CAD5 or L929, respectively, for the duration of each passage (~72hrs). For treatments, cells were passed at a 1:4.

Immunoblot Analysis

Confluent cells were washed twice in DPBS and then resuspended in 100μL of Radioimmunoprecipitation assay (RIPA) lysis buffer (150mM NaCl, 1% Triton X-100, 0.5% sodium deoxycholate, 0.1% SDS, 50mM Tris, pH 8.0). A Bicinchoninic Acid (BCA) Assay was used to determine protein concentration[91]. For PK treatment, an aliquot of the cell lysate (as determined by the BCA) was taken and digested with PK by incubating 20μg/mL for 1hr at 37°C and digestion was stopped by the addition of a proteinase inhibitor (1mM Pefabloc[92]) and incubation at 4°C for 15 minutes. Sample buffer (62.5mM Tris-HCl; pH 6.8, 5% glycerol, 5% SDS (sodium dodecyl sulphate), 3mM EDTA, 0.02% bromophenol blue, 4% β-mercaptoethanol) was then added from a 5X stock to a final concentration of 1X. Samples were then boiled at 100°C for 10 minutes and loaded into a precast NuPAGE (polyacrylamide gel electrophoresis) 4-12% Bis-Tris gradient gel (Fisher Scientific Cat: NP0321BOX). Immunoblots were run in a Novex Mini-Cell apparatus with NuPAGE MES running buffer (Fisher Scientific Cat: NP0002) at 150V for 1hr. Gels were then transferred to a polyvinylidene fluoride (PVDF) membrane (Fisher Scientific Cat: IPFL00010) with transfer buffer (1.9M Glycine and 245mM Tris base) in a Novex XCELL II blot module at 30V for 1hr. Membranes were blocked overnight at 4°C with

nonfat skim milk (5%) diluted in Tris-buffered saline (TBST – 0.1% Tween 20, 50mM Tris, 150mM NaCl; pH 7.8). Membranes were then probed by diluting the appropriate primary (1°) antibody in 5% nonfat skim milk at a 1:10000 (PrP and β-actin) or 1:5000 (LC3) at room temperature for 1hr. Membranes were then washed for 5 minutes three times with TBST, and then the appropriate alkaline phosphatase (AP) conjugated secondary (2°) (α-mouse (Promega Cat: PRS3721) for PrP and β-actin, α-rabbit (Fisher Scientific Cat: 31345) for LC3) diluted at 1:10000 in 5% nonfat skim milk was added and incubated at room temperature for 1hr. Membranes were then washed with TBST three times for 5, 10, and 15 minutes. After washing, membranes were developed using the Attophos System (Fisher Scientific Cat: S1000) for 5 minutes, then dried before imaging.

Statistical Analysis

Quantification of immunoblot signals was done using the ImageQuant TL program (ImageQuant Analysis, Molecular Dynamics). Statistical analysis was done using the Prism 7 software (Graphpad Software, San Diego, California). Statistical significance is noted by *$p<0.05$, **$p<0.01$, ***$p<0.001$, ****$p<0.0001$. LC3-II was measured relative to actin to determine autophagy levels.

Results

Characterizing the Basal Autophagosome Formation & PrP^C Expression of the Cell Lines

Cells derived from different lineages can be distinguished by their variance in protein expression levels. Even within a given lineage, sister cells can have variable protein expression. For example, in the central nervous system (CNS), neurons commonly express the protein NeuN, with the exception of a few subtypes of neurons (Golgi cells, Purkinje cells, etc.), while astrocytes express glial fibrillary acidic protein (GFAP). Since each cell can express different proteins at different levels depending on many factors (pH, cell-cell interactions, etc.), it is probable that different cell types express different levels of PrP^C. Furthermore, highly conserved metabolic processes, such as autophagy, may also vary in the degree of activity. Therefore, before the application of any pharmaceutical agent to modulate autophagy, it is necessary to establish the relative basal levels of autophagosome formation for each cell type.

To do this, L929, CAD5, N2a cells were chosen in order to model PrP^{Sc} infectivity in different cell lineages known to be receptive to prion infection. Cells were grown in a 6-well plate for 72hrs and then collected and probed for the autophagy marker microtubule-associated protein 1 light chain 3 (LC3-I/II), as well as actin as a loading control. Upon autophagic activation, cytosolic LC3-I (~16-18 kDa) is converted into LC3-II (~14-16 kDa) and can serve as a means to monitor autophagy through autophagosome formation [93] . **Figure 1a & 1b** shows immunoblot levels and associated densitometric analysis of LC3-II and actin for L929, CAD5, and N2a cells, respectively. On average, L929 cells have the highest basal level of autophagosome formation followed by CAD5 cells, with N2a cells having the lowest amount of basal autophagosome formation.

Since a supply of PrP^C is obligatory for prion replication [4] , it is also important to establish basal levels of PrP^C are in each of the various cell lines. When looking for PrP^C on an immunoblot, the signal is manifest as ~25, ~30, and ~ 35 kDa species corresponding to the un-, mono-, and di-glycosylated forms, respectively. On average, CAD5 cells have the highest levels of PrP^C relative to the other two cell lines, with L929 cells expressing significantly less PrP^C compared to the two neuronal cell lines (**Figure 1c & 1d**). Other studies that have evaluated PrP^C levels in L929 cells confirm the lower expression of PrP^C in this cell line [94] .

Autophagy in Cells Under Chronic Prion Infection

When cells are under stress, either from the accumulation of misfolded proteins as seen in prion infection or other cellular insults, they adjust their activities in order to cope. This is true for autophagy, especially in the case of protein misfolding diseases as this cellular housekeeping mechanism is one of the two main modes of riding the cell of misfolded proteins (the UPS being the other one). Thus, we predict that levels of autophagy under chronic prion infection should be increased in comparison to the basal autophagy levels.

Chronically infected cells, specifically CAD5-RML, were grown in a manner similar to above, then the cells were harvested after 72hrs and probed for LC3, actin, and PrP^{Sc} with the associated densitometric analysis (**Figure 2a**). With respect to autophagosome formation, we expected that there would be an elevation in autophagosome formation indicative of an elevated autophagic state, however there was no significant difference in autophagy in CAD5-RML cells compared to uninfected CAD5 cells (**Figure 2b**).

Attempting to Establish De Novo Infection in N2a & CAD5 Cells

Despite prion infection being persistent in some cell lines, establishing a new chronic infection in a cell line is not always a predictable process. To establish a chronic infection it takes many passages of the inoculated line and successive selection of the particular sub-clone(s) that carry the infection. It can take many months to establish a stable chronic infection.

To demonstrate this, cultures of N2a and CAD5 cell lines were exposed to RML BH at passage 1 and passed six times, collecting an aliquot of cells every passage. By definition, chronic infection would be demonstrated by steady persistent PrP^{Sc} signal in successive passages. Immunoblot analyses for PrP^{Sc} levels in *de novo* infected N2a (**Figure 3a**) and CAD5 (**Figure 3c**) cells were compared to an RML BH standard in order to determine relative protein quantities of PrP^{Sc}. Both cell lines showed a consistent reduction in PrP^{Sc} signal in a time-dependent manner (**Figures 3b & 3d**). The data demonstrates that even in lines that can be chronically infected, establishing a persistent infection is not guaranteed.

Curing Prion Infection From Chronically Infected Cells

It is known that there are different factors that contribute to cell susceptibility in prion infection, and one of these factors may be clonal variation, as cell to cell variations in expression of cell surface polyanion molecules or changes in membrane lipid content can influence prion propagation. Chronically infected cells may simply be a susceptible subclone of the parent cell line and variation between subclones of a given cell line, including relative PrP^C levels, can be a contributing factor to the hindrance of establishing a chronic prion infection. However, given that chronically infected cells can be cured using pentosan polysulfate (PPS), it would be advantageous to do so and test the cured cells for susceptibility to a *de novo* infection, potentially eliminating confounding factors associated with clonal variation.

To confirm that the CAD5 cells were cured, we compared an immunoblot of triplicate cured CAD5 samples with a CAD5-RML infected control and showed that the cured CAD5 cells had no detectable PrP^{Sc} signal after PK digestion. This indicated that PPS treatment cured the chronic infection (**Figure 4a**). Following this, cured CAD5 cells were re-inoculated with RML BH and passed six times to assess whether *de novo* infection could be established in cured cells. An aliquot was collected at each passage. Immunoblot analysis for PrP^{Sc} showed a decrease in PrP^{Sc} signal from P2 to undetectable levels at P6, similar to what was seen in control experiments of naïve CAD5 cells (above) (**Figure 4b & 4d**). Unlike the *de novo* infection experiments in naïve CAD5 cells, PrP^{Sc} levels in the cured CAD5 cell infection experiments were markedly lower in early passages. To determine a possible explanation for this, we compared PrP^C levels in uninfected CAD5, cured CAD5, and CAD5-RML by immunoblot analysis. We found a significantly lower level of PrP^C in the cured CAD5 cells compared to the uninfected CAD5 and CAD5-RML cell lines (**Figure 4c & 4e**). Other studies have reported that PPS can reduce the total amount of PrP^C available for conversion [95]. Therefore, the reduction in basal levels of PrP^C may explain why the transmission of RML into the cured CAD5 cells resulted in a lower persistence of detectable PrP^{Sc} compared to naive CAD5 cells, despite the cured CAD5 cells having previously maintained a chronic prion infection.

Autophagy in L929 Cells Under De Novo Prion Infection

Certain cell lines that can be infected with prions only maintain the infection for a short period of time. These cell lines are referred to as "acutely" infected cell lines, as the infection is cleared after a certain number of passages. Since it has been shown that autophagosome formation increases under prion infection, we predict that autophagosome formation increases over the course of a *de novo* infection in the L929 cell line.

Cultures of L929 cells were inoculated with RML BH at passage 1 and cultured for 72hrs, then split and passed for seven passages with each passage probed for LC3, actin, and PrP^{Sc}. The majority of *de novo* infected L929 experiments (7 of 11) showed an initial decrease in PrP^{Sc} signal from P2 until the signal was undetectable around P5 by immunoblot, followed by a re-emergence of the PrP^{Sc} signal in P6/7, albeit at lower signal levels than the original inoculum (**Figure 5a & 5c**). This recurrence of signal is indicative of a true *de novo* infection, and not an indication of the presence of residual inoculum. This reflects what is seen *in vivo*; animal models inoculated with infectious prion material show a significant reduction in detectable infectious prions as early as 24hrs post inoculation [96, 97]. The reasons for this observation *in vivo* are complex, and it may be that the absence of PrP^{Sc} only reflects an absence of PK-resistant prions; protease sensitive oligomers are infectious may persist during this period, allowing ongoing infection and later return of PK-resistant PrP^{Sc}. By contrast, in the remaining 4 of 11 experiments, PrP^{Sc} signal did not return after P5 and the efficiency of the infection, as defined by the persistence of PrP^{Sc} signal in later passages, was lower than the experiments where PrP^{Sc} returned (**Figure 5b & 5c**).

When monitoring autophagosome formation via changes in LC3-II/actin, an interesting pattern emerged in experiments where there was a re-emergence of PrP^{Sc} signal. Autophagosome formation was relatively low in P2 while PrP^{Sc} levels were still high, and then in subsequent passages, as autophagosome formation went up, PrP^{Sc} signal went down until it was undetectable. Upon clearance of PrP^{Sc} in P5, autophagosome formation was reduced and PrP^{Sc} began to re-emerge (P6/7). As the PrP^{Sc} signal returned, autophagosome formation began to increase once more (**Figure 5d**). For experiments where PrP^{Sc} signal did not return, there was a consistent elevation of autophagosome formation throughout the later passages (**Figure 5d**).

Autophagy has been shown to be beneficial in the clearance of misfolded PrP [87] . Many studies induce autophagy in an mammalian target of rapamycin (mTOR)-dependent manner (usually rapamycin) in order to clear misfolded PrP. Researchers have also shown that autophagic induction through an mTOR-independent mechanism can have the same beneficial effect, not only in the context of prion disease, but for other protein misfolding diseases [98, 99] . Along with this beneficial effect of reducing PrP^{Sc}, induction of autophagy should also protect against prion infection and reduce a cell's susceptibility to becoming infected. Since it is known that trehalose acts in an mTOR-independent manner and has been shown to be beneficial in prion infection in N2a cells [99] , we chose to investigate whether trehalose can also clear PrP^{Sc} in chronically infected CAD5 cells, and whether induction of autophagy can protect L929 cells against *de novo* prion infection.

For L929 cells, 100mM of trehalose caused adverse effects and drastically effected cell viability evident by the severe reduction in cell growth rate/proliferation (data not shown). Experiments with 10 and 50mM trehalose were performed; 50mM significantly induced autophagy but had also had a negative effect on cell viability, while 10mM did not significantly induce autophagy, so 25mM of trehalose was chosen as an intermediate between the two concentrations as this concentration was effective in inducing autophagy to a level significantly higher than the control, while also having no observable negative effects on cell growth (**Figure 6a-c**). To confirm that autophagic induction via trehalose was the cause for any reduction that may be seen in PrP^{Sc} and not simply because trehalose reduces the amount of available PrP^{C}, an immunoblot was run of control L929 cells compared with the trehalose treated cells, and no significant difference in the levels of PrP^{C} was found (**Figure 6d**).

We then confirmed that the 100mM concentration of trehalose used in previous studies of N2a cells was efficient in the induction of autophagy (**Figure 7a & 7c**). Since both N2a and CAD5 cells are neuronally derived, we hypothesised that the same concentration of trehalose needed to induce autophagy in N2a cells would be sufficient for CAD5 cells, and this assumption was confirmed experimentally (**Figure 7b & 7c**). An immunoblot looking at PrP^{C} levels indicated no significant difference in PrP^{C} levels in CAD5 cells in the treated vs. untreated conditions (**Figure 7d**). However, in contrast to previous studies [99] which showed no significant

difference in PrP^C levels in treated vs. untreated N2a cells, our experiments showed a significant difference, where there was more PrP^C in the treated cells and less in the untreated cells (**Figure 7d**). If anything, this increase in PrP^C levels in treated N2a cells could potentially negate the effects of trehalose by providing more substrate for conversion while autophagy induction is trying to clear newly formed PrP^{Sc}.

After determining the appropriate experimental concentrations of trehalose, cultures of L929 cells infected with RML BH at passage 1 and chronically infected CAD5-RML cells were subjected to the aforementioned concentrations of trehalose for longer durations to determine whether long-term treatment could reduce PrP^{Sc} levels in a time-dependent manner (3 passages for CAD5-RML, 7 passages for L929). Persistent trehalose treatment in the chronically infected CAD5-RML cells caused a significant reduction in PrP^{Sc} signal over the course of just three passages (**Figure 8a & 8b**). Quantification revealed that long-term treatment of L929 cells with trehalose eliminated the return of the PrP^{Sc} signal in P6/7 seen in control infected L929 cells, indicating that the induction of autophagosome formation increased the cells' resistance to the recurrent prion infection (**Figure 8c & 8d**).

Taken together, these results suggest that activation of mTOR-independent autophagy via trehalose leads to a time-dependent reduction of PrP^{Sc} in chronically infected cells and a reduction in the susceptibility of *de novo* infected L929 cells to prion infection as indicative of the elimination of the return of the PrP^{Sc} signal in P6/7. This is consistent with our hypothesis that increasing autophagy can reduce cell susceptibility to prion infection.

Autophagy Inhibition Using Wortmannin Increases Cell Susceptibility to Prion Infection In Neuronal Cell Lines

We have thus far demonstrated that chronic prion infection of N2a and CAD5 cells is difficult to establish, and that inducing autophagy can make cells less susceptible to *de novo* prion infection (L929), as well as help in the clearance of PrP^{Sc} in a chronic prion infection paradigm (CAD5-RML). Thus, if increased autophagy can reduce a given cell's susceptibility to prion infection, then reduction of autophagy via an autophagic inhibitor should increase a cell's susceptibility to prion infection, enhancing a *de novo* infection process. There are many chemicals that can inhibit autophagy, acting at different portions of the autophagic pathway [100].

For this experiment, we originally chose 3-methyladenine (3-MA), a PI3K inhibitor, to inhibit autophagy. However, recent studies have shown that in the presence of serum, 3-MA induces autophagy, having the opposite intended effect [90]. We then used another PI3K inhibitor, wortmannin, which can reliably and irreversibly inhibit autophagy in the presence of serum.

To determine the necessary experimental concentrations of wortmannin needed to reduce autophagic levels significantly, N2a, CAD5, and L929 cells were cultured either in the presence or absence of wortmannin at either 1μM or 10μM for 72hrs. 1μM was sufficient to inhibit autophagy significantly in the two neuronal cell lines (N2a & CAD5), while 10μM was necessary to inhibit autophagy in L929 cells (**Figure 9a-d**). PrP^C was also monitored to determine if treatment with wortmannin alters the amount of PrP^C. Immunoblot analysis revealed that there was no significant difference in PrP^C levels in N2a cells, but in the CAD5 cell line the 10μM concentration significantly reduced PrP^C levels, which would confound any findings by artificially reducing the amount of PrP^C available for conversion (**Figure 9e**). Additionally, treatment with wortmannin at the experimental concentration of 10μM caused a significant increase in PrP^C levels in L929 cells (**Figure 9e**). If this increase in PrP^C were to affect the experiment, we would expect that an increase in substrate available for conversion would make infections of these cells easier than untreated L929 cells.

Cultures of N2a, CAD5, and L929 cells were then exposed to RML BH at passage 1 and passed seven times, collecting aliquots at each passage. Only 1 of 6 N2a infection experiments showed PrP^{Sc} signal past P5 (**Figure 10a & 10c**) in contrast to 5 of 6 infection experiments that lost detectable PrP^{Sc} signal after P5 (**Figure 10b & 10c**), similar to the pattern seen in untreated N2a cell infection experiments. When LC3-II levels were examined in relation to actin they showed that for the one experiment where PrP^{Sc} signal returned after P5, there was a decrease in autophagosome formation between P2 and P3, while experiments where PrP^{Sc} signal did not return showed a consistent autophagosome formation between P2 and P3 (**Figure 10d**). From P4 onward, all 6 experiments followed the same pattern of relative autophagosome formation.

CAD5 cells exposed to RML BH at passage 1 demonstrated, in 4 of 9 experiments, a return of PrP^{Sc} signal after P5 (**Figure 11a & 11c**). In contrast, 5 of 9 experiments had a loss of PrP^{Sc} signal after P5 (**Figure 11b & 11c**), similar to the pattern seen in untreated CAD5 cell infection experiments. LC3-II levels in relation to actin showed that when PrP^{Sc} signal returned

after P5, there was a relatively stable autophagosome production in P2-P4 when compared to the experiments where PrP^{Sc} signal was lost after P5, in which there was a slight gradual elevation in autophagosome formation from P2-P4 (**Figure 11d**).

When L929 cells were treated long-term with wortmannin, 9 of 9 experiments showed no PrP^{Sc} signal (**Figure 12a & 12b**), in contrast to untreated L929 experiments (above) in which 7 of 11 returned with positive PrP^{Sc} signal. When LC3-II levels in relation to actin were examined, there was a decrease in autophagosome formation between P2 and P3, followed by a gradual increase in autophagosome formation from P3 to P6 (**Figure 12a & 12c**).

Discussion

The incidence of neurodegenerative diseases increases with age. Due to an increase in the lifespan in industrialized societies, neurodegenerative diseases are becoming more and more common. As people age, normal cellular process such as autophagy start to become dysfunctional and can lead to an increase in tissue degeneration in the CNS and throughout the body [101]. Many studies have supported autophagy as a key mechanism for clearance of aggregated misfolded proteins implicated in many of these diseases, including huntingtin (Huntington's disease), α-synuclein (Parkinson's disease), amyloid-β and tau (Alzheimer's disease), and of course, PrP (Prion disease(s)), and therefore autophagic impairment may lead to an increase in the prevalence of these neurodegenerative diseases as people age [71, 102].

In the context of prion disease, it has been demonstrated in previous studies that different prion strains present with varying spongiform/neuropathological profiles, which can be explained, at least in part, by the different cells types present [59, 103]. Different cell types possess different characteristics, from cell morphology to protein expression levels, and these differences can contribute to a given cell's susceptibility to infection from any type of agent, including prions. Therefore, it is important to determine which cellular processes(s) contribute to their relative susceptibility to infection from prions. This study focused on autophagy, aiming to determine the differences in basal autophagy levels between cell lines and whether this plays a role in prion susceptibility. Additionally, this study tried to determine if it is possible to alter cell susceptibility to prion infection through modulation of autophagy.

Methods for Monitoring Autophagy & Comparing the Basal Autophagy Levels Between Different Cell Lines

Autophagy is an evolutionary conserved mechanism from yeast to mammals that aids the cell in the reduction and clearance of unwanted cellular organelles, cellular debris, and misfolded proteins. The autophagic process has a lot of crosstalk with other cellular mechanisms relating to homeostasis (UPS) and programmed cell death (apoptosis) and many of the proteins involved with initiation and/or execution of autophagy play roles in these other pathways [71, 72, 104]. In addition, autophagy has been shown to be a major pathway for many misfolded proteins

associated with neurodegenerative diseases [105]. Therefore, the proper monitoring of autophagy requires careful selection of cell markers.

The most common autophagic marker, and the one used to monitor autophagy in this study, is LC3. LC3 undergoes post-translational modification by cleavage of the C-terminal resulting in the cytosolic LC3-I form. LC3-I is then conjugated to phosphatidylethanolamine (PE) by Atg7 (E1 ubiquitin-activating enzyme-like) and Atg3 (E2 ubiquitin-conjugating enzyme-like) to create the autophagosome associated LC3-II [106]. Its primary purpose in autophagy is to mediate membrane tethering and expansion and eventual closure of the phagophore, resulting in the formation of the autophagosome [107]. Since LC3-II remains associated with the autophagosome, both on the interior and cytoplasmic surfaces, LC3-II correlates with the number of autophagosomes [106]. When measuring LC3 levels, a good correlation of the levels of autophagosome formation is to take the relative amount of LC3-II and compare it to a protein that remains unchanged, like actin. A larger ratio of LC3-II/actin is indicative of a higher rate of autophagosome formation, and likely a higher rate of autophagic flux [108]. Other studies have monitored relative levels of proteins that are upstream of LC3, such as Beclin-1 (an orthologue of the yeast Atg6), mTOR activity, and phosphorylation of serine/threonine protein kinase (ULK1), among others [108]. The issue with some of these proteins with respect to autophagic monitoring is that they are either involved in other cellular processes related to cell death and/or they aren't involved at all under certain autophagic conditions. For example, autophagy can proceed independent of mTOR, as seen with the chemical agonist trehalose [99]. Beclin-1 interacts with several cofactors involved in autophagy (Ambra1, PINK, Atg14L, etc.) but also has a BH3 domain that is bound to, and inhibited by, the anti-apoptotic protein Bcl-2, which can be disrupted by phosphorylation of Bcl-2 or ubiquitination of Beclin-1 [109].

Given that different cell types exist to perform different functions, it follows that they may differ in the repertoire and levels of expression of proteins relevant to neurpathogenesis. Morphologically, L929 cells are an adherent cell line derived from subcutaneous connective tissue of mice that have fibroblast-like shape [110] (flat, large, and elongated (spindle-shaped) cells possessing processes extending out from the ends of the cell body). N2a and CAD5 cells are both adherent cells derived from tumours, with N2a cells coming from a murine neuroblastoma and the CAD5 cells originating from murine catecholamingeric neuronal

tumours. Despite both cell lines being neuronally derived and expressing neuronal properties, they differ in many respects. For instance, N2a is an immortalized cell line possessing classic neuromorphology (dendrites and axons), while CAD5 cells lack neuronal morphology [111]. In addition, N2a cells are strongly adherent to cell culture flasks, requiring the use of trypsin to lyse their adherence molecules, whereas CAD5 cells only require moderate fluid force to detach them from cell culture plates (observations from this study). It is important to note that for experimental procedures, cells were removed from the plate with a cell scraper and not trypsin, as trypsin strips surface proteins, including PrP^C, and could lead to an underestimation of how much PrP^C is actually present. Finally, under serum rich conditions CAD5 cells remain undifferentiated, where upon serum starvation they differentiate, whereas N2a are fully differentiated [111].

Figure 1 outlines the basal levels of autophagy and PrP^C expression. L929 cells have a higher basal level of autophagy compared to the neuronal-based cell lines. This elevated basal autophagy in relation to the two neuronal cell lines tested may contribute to the L929 cells' low susceptibility to *de novo* infection. There is also a difference in basal autophagosome formation between N2a and CAD5 cells in this study, with CAD5 cells, on average, having a higher level of basal autophagosome formation in relation to N2a cells. With respect to PrP^C levels, L929 cells have significantly less PrP^C than the two other lines on average, and this significant reduction in PrP^C may also contribute to the relative difficulty in establishing an infection.

Changes in Autophagy After Prion Infection

Cells undergoing prion infection, whether *de novo* or chronic, experience stress from a build-up of misfolded PrP. Misfolded PrP can be present in the cytosol, however the majority of PrP^{Sc} is found on the surface of the plasma membrane and in vesicles associated with the endo-lysosomal system, the Golgi and *trans* Golgi network, and the autophagic pathway [112-114]. The increase in the presence of misfolded proteins will cause an upregulation of intracellular mechanisms, namely the ER-associated degradation pathway (ERAD), UPS, and autophagy, to rid the cell of these insults. The UPS is responsible for the breakdown of over 80% of abnormal intracellular proteins [115, 116]. However, this process of proteasomal degradation can be restricted to smaller oligomeric forms of PrP^{Sc} that can fit into the barrel of the catalytic chamber of the proteasome (entrance can be as narrow as 13Å), whereas larger, more insoluble aggregates may

not have access, impairing the UPS and preventing the effective breakdown of misfolded proteins [117]. Misfolded PrP in the oligomeric form is known to interact with the proteasome and impair the function of the catalytic β-subunits of the 20S proteasome [118]. Other studies have shown that β-sheet rich PrP can reduce gate opening of the proteasome and inhibit substrate entry [119]. The immediate consequence of ERAD/UPS inhibition is an increased burden on the autophagic system, as studies have shown that impairment of the ERAD/UPS induces an upregulation of autophagy as a compensatory mechanism [120].

In this study, the data demonstrates that cellular levels of autophagosome formation, on average, do not increase under *de novo* prion infection when compared to basal levels, and in some cases may be lower than uninfected controls. This is in contrast to what is observed in other studies, which show an overall increase in autophagosome formation [121]. Additionally, we found that the autophagosome formation rate was relatively similar in chronic infected cell line (CAD5-RML) compared to the uninfected cells (**Figure 2**). However, if we compare the change in autophagy over time in *de novo* L929 infections, there was a significant difference in autophagosome formation between early (P2-4) and late (P5-7) passages, and the pattern of change in autophagy rates depended on whether there was a return in PrP^{Sc} signal in late passages (positive) or not (negative).

In *de novo* prion infection, there is an increase in protein burden on the cell, which can be predicted to overwhelm the ERAD/UPS causing early impairment [122], which likely triggers an increase in autophagy. This is in fact what we saw in the *de novo* L929 infections (**Figure 5**); PrP^{Sc} signal initially declined in P2-3 without an associated change in autophagy, suggesting that other clearance mechanisms were in play, or conversion was inefficient. However, the majority of *de novo* L929 infection experiments saw a return of PrP^{Sc} signal in later passages, which excludes the possibility of inefficient conversion. Therefore, this "lag time" between a decline in PrP^{Sc} signal and an increase in autophagosome formation suggests that initially the cell employed other means of clearance, likely the ERAD/UPS. As PrP^{Sc} signal continued to decline in the first 4 passages, autophagosome formation actually increased until P4, where the increase in the rate of autophagosome formation was significantly elevated from the rate observed in P2. In P5 when PrP^{Sc} signal was undetectable by immunoblot, autophagosome formation was still significantly higher than in P2 but then started to decline in relation to P4, indicating a reduction

in autophagy. By P6, the rate of autophagosome formation was no longer significantly different from the levels of formation in P2. This reduction in autophagosome formation may have been enough to allow some PrP^{Sc} to escape complete clearance, allowing for the re-emergence of the infection. In P7 the autophagosome formation increased once again, but with a reduction in lag time between PrP^{Sc} formation and autophagosome production than that seen after the initial inoculation. This elimination of lag time in relation to increasing PrP^{Sc} signal suggests that the UPS was still dysfunctional, indicating that the amount of misfolded PrP present was still able to inhibit the UPS, even if the PrP^{Sc} signal was undetectable by immunoblot.

In contrast, experiments with L929 cells where PrP^{Sc} signal did not return in late passages, autophagosome formation remained elevated (in relation to P2) significantly in late passages, following presumed UPS impairment. These results suggest that upon prion infection, there is a tipping point in the course of infection where autophagy becomes a more important regulatory mechanism than the UPS with respect to combating prion infection due to the ability of misfolded PrP to inhibit UPS function. Additionally, decreasing autophagosome formation, even briefly, can allow for the re-emergence of infection, but sustained elevation of autophagosome formation in late passages relative to early passages allows for a more complete clearance of PrP^{Sc}, which prevents the establishment of a *de novo* infection in *de novo* infected L929 cells. This supports our initial hypothesis that an upregulation of autophagy in early passages can help clear cells of misfolded PrP and that sustaining an elevated autophagic state can inhibit the return of misfolded PrP in late passages.

Barriers to Prion Infection and the Creation of Chronically Infected Cell Lines

Despite the insidious nature of prion diseases, establishing prion infection in any particular cell line is no easy task. There are many different factors that contribute to a cell's susceptibility to prion infection, including the focus of this study, autophagy. Different aspects of PrP^C itself can affect the degree of prion susceptibility, including the tertiary structure and relative levels of expression. As mentioned above, the absence of PrP^C confers complete resistance to prion infection[4]. In addition, according to the cloud hypothesis proposed by Collinge and colleagues, transmission between and within species is largely dependent on the shape the misfolded PrP[54]. Due to these limitations, most of the cell lines derived from mice are only susceptible to prions that are murine-based, however there are recent adaptions to allow for

expression and susceptibility to cervid prion diseases [66, 123-125]. Currently there are no chronically infected cell lines that can replicate BSE or CJD material without first being adapted to mice; for one reported instance of a human-derived neuroblastoma cell line propagating CJD prions the cell line proved unstable and has subsequently been lost [126, 127].

The reasoning behind the variation in susceptibility to different prion strains by different cell lines is unclear, but has to do with a balance between conversion, degradation, state of differentiation, and cell division [128]. When a cell line possesses a high rate of cell growth/division and/or elevated basal autophagy levels in compared to other cell lines, the growth rate will outpace the replication of misfolded PrP, and persistent infection is usually lost after continuous passages [129, 130]. In addition, changes in culture media composition and conditions can also have a drastic effect on prion replication [67]. These aspects also apply to chronically infected cell lines, but there are other issues from which certain neuronally derived chronic cell lines suffer. The main neuronal cell line used in prion infection assays is the N2a cell line, due to its susceptibility to a variety of prion strains [66, 67, 129]. CAD5 cells are also quite susceptible to a wide variety of prion strains. As mentioned, both cell lines have neuronal characteristics and are tumour derived, allowing for consistent growth and division, however there are negative consequences to this. Due to the nature of tumours, most tumour lines suffer from genetic instability [131]. The N2a cell line suffers from severe chromosomal instability, where chromosomal number can vary from as low as 59 to as high as 193 and this genetic instability can cause variation in PrP^C/PrP^{Sc} levels, making it difficult to interpret results [132]. This instability can also cause spontaneous loss of prion infection in chronically infected cells. For these reasons, it can be extremely difficult to establish a chronic prion infection.

In this study, establishment of a chronic prion infection was attempted in naive N2a and CAD5 cells, as well as CAD5 cells that were cured of a chronic prion infection. When inoculated with prions at P1, N2a and CAD5 cells failed to maintain the infection past P5, demonstrating how difficult it is to create chronically infected cells (**Figure 3**). In direct opposition to our initial hypothesis, none of the *de novo* infection experiments in N2a or CAD5 cells were positive for PrP^{Sc} material in late passages, while more than half of the L929 *de novo* infection experiments had positive PrP^{Sc} in late passages (above section), despite L929 having the highest relative levels of autophagy.

In order to create a chronic line, infection is done in a similar way to this study, but cells are selected for passage based on the degree of susceptibility to prions. The majority of cells in any given culture will be resistant to prion infection, but a subset (<1%) of the population will have genomic variations that render these particular cells more permissive to prion infection [133-135]. These cells are then selected from the general population and passed until the culture is comprised of a specific clonal variant of the original population that has the ability to maintain a stable and persistent infection [136].

When a cell line becomes persistently infected with prions, some chemicals that have been shown to have anti-prion activity can cure these cells of the chronic infection. One of these is pentosan polysulfate (PPS) and it functions by stabilizing PrP^C and inhibiting conversion into PrP^{Sc} [137]. We used PPS to cure persistently infected CAD5-RML cells of the RML infection, referred to as cured CAD5. The rationale was to cure the cell line and attempt to re-infect this line with the same agent, which would remove the variable of clonal differences that may exist between the persistently infected CAD5-RML cell line and the naïve CAD5 cell line. Surprisingly, we found that re-infection of these cured CAD5 cells was less efficient than *de novo* infection of naïve CAD5 cells (**Figure 4**). This is in contrast to other studies that report that SMB cells cured with PPS were able to be re-infected with either the same inoculum or even different prion strains [138]. As revealed by immunoblot, we showed that cured CAD5 cells had less PrP^C than either the naïve CAD5 cells or the persistently infected CAD5-RML cells. Since PrP^C is necessary for PrP^{Sc} conversion, the reduction in PrP^C could explanation the relative difficulty in re-establishing the chronic infection. In addition, since the RML inoculum used in this study was from a different batch used to establish the initial chronic infection, it is also possible that infectious material per unit of volume is a relevant operational variable.

Induction of Autophagy: the Effect on Cell Susceptibility & Cellular Levels of PrP^{Sc}

There are many studies that show that inducing autophagy can be beneficial in the clearance of PrP^{Sc}, not only in cell culture, but also in animal models of prion disease [90, 99, 139-141]. These studies used a variety of chemical inducers, from rapamycin to lithium to trehalose. In this study, rapamycin was originally chosen to induce autophagy, but after many experiments it was clear that rapamycin was not ideal. The rationale for selecting a different drug was three-fold: 1) rapamycin acts only on mTORC1 and has very little effect on mTORC2, which may

confound interpreting results because inhibiting mTORC1 can activate mTORC2 [142] , 2) mTORC2 plays a large role in cancer [142] , and 3) the efficacy of rapamycin varied significantly between and within experiments and the results were not consistently replicable (data not shown). Additionally, experiments show that neurons may differ from other cells in both mTOR-dependent and mTOR-independent modes of autophagy [143] . Trehalose, an mTOR-independent chemical agonist of autophagy, was then chosen because of its proven efficacy and potency of autophagic induction in the N2a cell line [99] . Trehalose increases autophagic flux by inducing a starvation-like state independent of nutrient intake [144] . Studies indicate that trehalose induces this state by inhibiting glucose transporters (GLUT1, GLUT2, GLUT3, GLUT4, and GLUT8) at the plasma membrane, resulting in AMPK activation and subsequent phosphorylation of ULK1 [145] . There are confounding factors when using trehalose, as it has been shown that it does not readily cross the cell membrane, but enters the cell via endo/pino-cytosis [98] . This can hinder its efficacy if these cellular transport mechanisms are impaired in the cell line under investigation. In addition, work by Béranger and colleagues suggest that trehalose can also prevent formation of *de novo* PrP^{Sc} aggregates, but does not dissociate existing aggregates [146] . It has been proposed that the mechanism by which trehalose reduces aggregation is by isolating water molecules in the layer surrounding the protein, preventing hydrophobic regions from burying themselves in the protein structure [146, 147] .

Previous studies in cell culture have shown that 100mM of trehalose significantly induces autophagy, can significantly reduce PrP^{Sc} levels at 48, 72, and 96h time points, and has no effect on cellular levels of PrP^{C} [99] . At this concentration there is no significant difference in cell viability as determined by trypan blue exclusion assay [99] . In addition, trehalose is added directly to the culture media as a powder, and is stable in solution for up to a month. This study replicated these parameters and found the same results in N2a cells with respect to the change in autophagy and stability of PrP^{C} levels. However, when using the chronic RML infected N2a line (ScN2a) in this study, there were large fluctuations in PrP^{Sc} levels from passage to passage, making results difficult to interpret. Therefore, we excluded using the ScN2a cell line from further experiments.

Both N2a and CAD5 cells are tumour cell lines derived from neuronal origin, can be chronically infected, and might therefore have similar reactions to chemical agents. Using the

100mM concentration of trehalose in CAD5 cells confirmed this, as there was a significant increase in autophagy with no adverse effects on PrP^C levels or cell viability (**Figure 7**). In previous studies, ScN2a treated with 100mM trehalose for up to 14 days resulted in reduction of PrP^{Sc} signal to an undetectable level via immunoblot. In this study, a similar trend of PrP^{Sc} signal elimination was observed when persistently infected CAD5-RML cells were treated for 3 passages (equivalent to 12 day - 4 days/passage). PrP^{Sc} levels were relatively equivalent after 96hrs (passage 1) in the presence of trehalose in relation to controls, and only significantly differed in P2 and P3. Interestingly, there was some variation within each passage in the control CAD5-RML cells, but the presence of trehalose decreased this variation in PrP^{Sc} signal (**Figure 8a & 8b**).

There are limited reported studies for L929 cells treated with trehalose and the majority of these centre on using trehalose as a method for cryopreservation and protection against electrotransfection [148, 149]. To our knowledge, this study is the first to use trehalose as a means to clear misfolded PrP from L929 cells. L929, unlike N2a and CAD5 cells, are not neuronally derived and divide rapidly. In the absence of trehalose, when L929 cells were inoculated with prion infected brain homogenate at first passage, they showed a progressive clearance of the prion material over the course of the early passages to the point where the PrP^{Sc} signal was essentially undetectable by immunoblot (**Figure 8c & 8d**). However, the signal returned in late passages, indicating a *bona fide* prion infection. Induction of autophagy in L929 cells required a much lower concentration of trehalose (25mM vs. 100mM for CAD5/N2a), and this may be due to L929 having a higher level of basal autophagy, indicating that this cell line may be more sensitive to autophagic augmentation (**Figure 6**). When cells were inoculated and passed in the presence of trehalose, there was a noticeable decrease in PrP^{Sc} signal in late passages relative to the control cells. This data demonstrates that consistent and prolonged induction of autophagy can be beneficial in L929 cells, and to a certain extent, can protect these cells from the re-emergence of PrP^{Sc} signal seen in the late passages of untreated control L929 infection experiments (as described above). These results support our hypothesis that prolonged induction of autophagy can reduce a cell's susceptibility to prion infection.

Inhibition of Autophagy: the Effect on the Cell Susceptibility and Cellular Levels of PrP^{Sc}

In contrast to induction of autophagy, inhibition should have the opposite effect. Given the importance of autophagy to cell development, it is not possible to completely eliminate this process from living animals; attempts to do so have proven to be embryonically lethal [150, 151]. It is possible to knock out genes related to autophagy in neural specific tissue, but these mice develop progressive motor defects and neurodegeneration [152]. To date, there are many chemical inhibitors of autophagy but the majority focus on two steps in the autophagic process – autophagosome formation and the lysosome [100]. Since this study focuses on LC3, which is indicative of autophagosome formation, we chose a chemical that blocks autophagosome formation (as opposed to lysosome function/fusion). The majority of autophagic inhibitors that block autophagosome formation do so through inhibition of class III phosphoinositide 3-kinase (PI3K). The main three PI3K inhibitors used in research are 3-methyladenine (3-MA), wortmannin, and LY294002. 3-MA was the first inhibitor to be identified and is the most ubiquitously used in research [153]. In the context of this study, 3-MA is not a suitable inhibitor due to having opposite effects depending on the presence of serum in the media, where an absence of serum allows for 3-MA to function as intended, however under serum rich conditions 3-MA induces rather than inhibits autophagy [90, 154]. 3-MA has been shown to persistently block class I PI3K (inhibitor of autophagy) and has transient effects on class III PI3K (activator of autophagy), while wortmannin persistently inhibits class III in a irreversible manner [154, 155]. Since wortmannin reliably inhibits autophagy, it was selected as the chemical inhibitor.

The three cell lines were treated with either 1μM or 10μM wortmannin for the duration of each passage (72hr) supplemented in the culture media (**Figure 9**). Interestingly, the concentrations needed for trehalose to induce autophagy in a cell line were inversely correlated to the concentrations needed to inhibit autophagy, with N2a/CAD5 cells needing more trehalose to induce autophagy than L929 (100mM vs. 25mM), but L929 needed more wortmannin to inhibit autophagy than N2a/CAD5 cells (10μM vs. 1μM). This correlation is possibly attributed to the basal level of autophagy that these cell lines possess; L929 cells have a high level of basal autophagy and therefore require less agonist to induce it and more antagonist to inhibit it, while N2a/CAD5 have relatively lower levels of basal autophagy and need more agonist to induce and less to inhibit.

In this study, we inoculated the three cell lines in a manner similar to previous experiments, and cultured them in the present of wortmannin over 7 passages. When we looked at the relative susceptibility to prion infection, as measured by the level and presence of PrP^{Sc}, we noted some interesting observations. First, for N2a cells infected in the presence of wortmannin, we observed 1 of 6 experiments return positive for PrP^{Sc} signal in late passages, compared to 0 of 6 experiments without wortmannin. Additionally, in CAD5 experiments supplemented with wortmannin, 4 of 9 experiments return positive for PrP^{Sc} signal in late passages, compared to 0 of 6 experiments without treatment. L929 cells supplemented with wortmannin resulted in 0 of 9 experiments returning positive for PrP^{Sc} signal in late passages, in contrast to 7 of 11 experiments without treatment. N2a and CAD5 experiments matched what we predicted; culturing cells in the presence of wortmannin after exposure to RML BH rendered them more susceptible to prion infection. Treatment of L929 cells with wortmannin, however, resulted in the exact opposite of what we predicted, rendering L929 less susceptible to prion infection compared to untreated controls.

Looking at the relative levels of LC3-II in relation to actin in N2a and CAD5 cells, there was no significant change in the ratios in experiments where PrP^{Sc} signal returned in late passages compared to experiments where PrP^{Sc} signal did not return in late passages. However, the change in autophagy levels over serial passages had different patterns in the positive and negative groups.

In the N2a experiments (**Figure 10**), there was one positive for PrP^{Sc} in late passages and this showed a decline in autophagosome formation in early passages (specifically between P2-P3). In contrast, the remaining experiments that were negative for PrP^{Sc} in late passages had no significant change in early passages, but instead, showed a significant reduction in autophagosome formation in late passages. This is possibly due to the relative stability of autophagosome formation in early passages, which may have been sufficient enough to clear the majority of PrP^{Sc}, so any reduction in autophagosome formation in late passages had a negligible effect on the return of PrP^{Sc} signal.

In the CAD5 groups (**Figure 11**), the 4 experiments that came back positive for PrP^{Sc} in late passages showed a steady state of autophagosome formation, only differing significantly in late passages (P6), where there was an increase in autophagosome formation. In contrast, the 5

experiments that came back negative for PrP^{Sc} in late passages had a significant increase in autophagosome formation in early passages, as well as late passages, similar to the positive experiments.

In the L929 groups (**Figure 12**), in all 9 experiments that were negative for PrP^{Sc} signal return in late passages, there was no significant change in autophagosome formation.

When taken together, the results indicate that long-term wortmannin treatment was not effective in reducing autophagosome formation; rather, in some cases, such as CAD5 cells, it significantly increased autophagosome formation. This led us to believe that wortmannin was either ineffective at reducing autophagosome formation significantly at the concentrations selected, or that it degraded over time. Other studies using wortmannin treated cells for up to 48hrs while still seeing efficacy and observing less than 10% cell death [156]. In addition, we performed initial experiments that showed wortmannin was able to significantly reduce autophagosome formation in each of the cell lines at the concentration tested after 72hrs of treatment.

We then researched the stability and half-life of wortmannin to determine whether it degrades over time, which would explain the lack of efficacy and relative increase in autophagosome formation. Indeed, although wortmannin is stable in powder form at 2-8°C for up to 3 years, and reconstituted in solution with dimethyl sulfoxide (DMSO) at -20°C for up to 3 months, once in aqueous solutions of between pH 3-8, the half-life of wortmannin is reduced to minutes [157]. Our culture media used for experiments is at a pH of 7.4 and was supplemented with wortmannin and aliquoted and stored at 4°C, with some aliquots used weeks after initial supplementation (similar to the supplementation and storage of media containing trehalose). It is possible that the wortmannin degraded in the culture media, which would explain why in most experiments across all 3 cell lines we saw a significant increase in autophagosome formation in later passages. In addition, it is possible that the reduction in autophagosome formation was not biologically significant. The difference between statistical and biological significance is that statistics give a probability that any differences seen are unlikely to have occurred by chance, whereas biological significance accounts for the importance of a result when compared to a "normal" biological state [158]. Taken together, our results neither confirm nor refute our

hypothesis that inhibition of autophagy can increase cell susceptibility, as the agent used for autophagic inhibition was inefficient in our experimental design.

Outside of this technical issue, there is evidence that supports the importance of autophagy in early passages but not late passages. By comparing autophagosome formation within positive and negative experiments, we observed distinct patterns. In the positive N2a infection experiment, autophagosome formation was reduced in early passages, whereas there was no change in autophagosome formation in the negative infection experiments. In the negative CAD5 infection experiments, autophagosome formation was increased in early passages and late passages (P6), whereas positive infection experiments only had an increase in autophagosome formation in late passages (P6). Therefore, a decrease in autophagosome formation, at least in N2a and CAD5 cells, in early passages may lead to an increase in susceptibility to prion infection, whereas an early increase in autophagosome formation may decrease susceptibility. Interestingly, L929 cells had no significant change in autophagosome formation across the 7 passages, yet none of the experiments resulted a return of PrP^{Sc} signal in late passages. This result is puzzling because if wortmannin was a non-factor due to its degradation as we postulate, then at least some of the experiments should have theoretically resulted in positive PrP^{Sc} signal in late passages, similar to control infections.

Other Factors That Influence Cell Susceptibility to Prion Infection

Genetics

There are clearly other factors outside of autophagy that cells possess that contribute to susceptibility to prion infection. First and foremost are genetic factors, specifically in the amino acid composition of PrP and the polymorphisms therein, combined with the numerous possible mutations, all of which affect the final conformation of the prion protein. Some mutations can confer resistance to prion disease, like the G127V polymorphism [52], while the vast majority of mutations increase susceptibility to development of various prion diseases [159]. In a study by Marbiah and colleagues, an investigation into a gene regulatory network using differentially susceptible subclones of the N2a cell line known as PK1 cells (~1000-fold more susceptible to infection [160]), resulted in the discovery of over 100 genes that varied in expression levels [161]. Many of the genes are involved in cell differentiation and development and the predominant

over-expression of genes in the susceptible cell line promote a differentiated phenotype [161] . Using shRNA-mediated knockdown, they found that knockdown of one of nine genes in the prion-resistant cells rendered these cells significantly more susceptible to prion infection. These genes include fibronectin 1 (Fn1), interleukin 11 receptor alpha chain 1 (Il11ra1), and galactosyltransferase (Galt), among others [161] . Interestingly, it was found that several of these proteins are associated with the extracellular matrix (ECM), indicating that the ECM plays a critical role in cell susceptibility [161, 162] .

Co-factors

Outside of genetics and tertiary structure, there are cellular co-factors that can aid in the conversion of PrP^C to PrP^{Sc}. These co-factors include, but not limited to, polyanions (RNA molecules and proteoglycans), lipids, and chaperones (heat shock protein 104 (Hsp104)) [47, 48, 163-165] . A study found that PrP^{Sc} amplification was enhanced with single stranded RNA (ssRNA) *in vitro*, but not double stranded RNA (dsRNA) or RNA:DNA hybrids [47] . This is consistent with findings that nucleic acids promote conformation change by binding to recombinant PrP [166] . Sulfated glycosaminoglycans (GAGs) exogenously applied are a potent inhibitor of prion propagation in cultured cells and animal models [137] . Lipids play a significant role as they can cause an approximate 100-fold increase in prion infectivity when purified PrP is re-incorporated into liposomes [48, 58] . As a chaperone, it was demonstrated that Hsp104, but not Hsp40/70/90, was able to convert PrP^C to PrP^{Sc}, although it required partial denaturation with urea [163] .

Post-translational Processing

In addition to these cellular co-factors, the post-translational processing (truncation, trafficking) of PrP^{Sc} can also influence cell susceptibility. It was demonstrated in a study by Jeffrey and colleagues of sheep with natural scrapie that there were two distinct scrapie strains present in the animals and that the pattern of PrP^{Sc} accumulation and associated subcellular lesions were present in both, however they differed in proportion [167] . This difference in deposition suggests that trafficking of PrP^{Sc} is influenced by both strain and cell type, and that a single prion strain (natural scrapie) can be differentially trafficked based on interactions at the cell membrane [167, 168] . The product of truncation can also affect trafficking and incubation time of the disease in relation to cell type. In transmissible mink encephalopathy, N-terminally

truncated PrP^{Sc} in the soma of neurons, astrocytes, and microglia resulted in short incubation periods, while N-terminally truncated PrP^{Sc} in glia but not in the soma of neurons produced longer incubation periods [169].

<u>Links with Autophagy</u>

Some of the above factors have roles in autophagy, namely the ECM and lipids, highlighting how certain factors that affect cell susceptibility through other means can also have an impact on autophagy to further modulate cell susceptibility. Lipids affect autophagy in more ways than one; they regulate the signal cascade(s) that converge on mTOR, they control membrane dynamics through acting as membrane-bound signal by recruiting cytosolic protein effectors that mediate expansion and vesicle transport, as well as being required for the conversion of LC3-I to LC3-II (via PE, a phospholipid) and anchoring LC3-II to the membrane of forming autophagosomes [170, 171]. Certain constituents of the ECM can modulate autophagy through interaction with specific receptors, thereby modifying autophagic signalling pathways. For instance, the C-terminus of perlecan (a type of heparan sulphate proteoglycan) known as endorepellin can induce autophagy in endothelial cells [172, 173]. In the context of prion disease, intestinal epithelial cells can accumulate PrP^{Sc} in orally infected animals, and brain endothelial cells express PrP^{C} as a junction protein that contributes to the composition of the blood-brain-barrier (BBB) [174, 175]. Recently it has been shown that the size of the N-terminally truncated PrP^{Sc} plays a role degradation and clearance. In studies comparing two strains of TME, namely drowsy (DY) and hyper (HY), researchers were able to demonstrate that if the strain under investigation is processed into a smaller truncated PrP^{Sc} (DY), it was more susceptible to degradation and clearance than other strains where the product of truncation is relatively larger (HY) [176]. This difference in processing and clearance could explain the differences in incubation times, with DY having a long incubation time when inoculated intercerebrally (~170 days) relative to HY (~60 days) [176].

In this study we used N2a and CAD5 cells as models for chronic infection, while using L929 cells as a model for *de novo* infections out to P7. Studies have shown through cloning that L929 cells are able to maintain detectable levels of PrP[Sc] past passage 12, and even as far as +15 passages for other fibroblast cell lines (NIH/3T3)[94]. These infections can faithfully propagate scrapie infections, as indicated by the inoculation of mice with cell lysates from passage 13 of NIH/3T3 cells that had been infected with 22L at passage one, where all mice inoculated died of clinical scrapie, although the incubation time was slightly longer (~185 days) than mice inoculated with 22L BH (~162 days)[94]. Since these cells can maintain a *bona fide* infection for longer durations, it is possible to extend the study of fibroblast to determine how autophagic manipulation can affect PrP[Sc] clearance over a longer period of time.

The initial premise of this work was to support the hypothesis that autophagy is beneficial in the degradation and clearance of PrP[Sc]. However, there is now recent evidence that may implicate autophagy in the spread of infectious prions. We discussed in earlier sections that misfolded PrP could be present on the surface of the cell, in endosomes associated with the endo-lysosomal pathway, and autophagosomes. In addition, depending on the pathway by which PrP[Sc] is N-terminally truncated, distinct glycoforms of PrP[Sc] can be incorporated into exosomes[177]. Furthermore, there has been evidence that supports that stimulating the release of exosomes aids in the spread of prions intercellularly[178]. Recently, some research shows that autophagy can stimulate the release of the exosomes, spreading infectious prion material between cells, counter to much of the evidence supporting autophagy as beneficial in prion disease[179].

In the future, experiments requiring long-term PI3K inhibition should be done with LY294002. Although LY294002 is less potent than wortmannin, it works in a similar manner and is much more stable in aqueous solutions[157]. Due to its high stability in solution, long-term treatment with this drug would likely result in a more consistent PI3K inhibition and therefore more consistent results. If this showed that inhibition of autophagy could make cells more susceptible to prion infection, it could aid in the development of new cell lines that can be infected to better model prion disease. An interesting point to consider is that in addition to modulation of autophagy to allow for a wider range of prion susceptible cell lines, it might be worth trying to infect cells that do not usually replicate prion infectivity *in vivo*. For instance, the

L929 cell line is a fibroblast cell line; fibroblasts do not replicate infectious prion material *in vivo*, but are clearly able to replicate and propagate infectious material *in vitro*[94]. Therefore, there may be other susceptible model cell lines available that have so far been overlooked because the tissue of origin does not replicate infectivity *in vivo*.

It would also be useful to test other strains in the three cell lines studied to determine whether modulating autophagy has a similar result. If other strains are found to have a similar response to autophagy manipulation, it would indicate that cell type plays a larger role in cell susceptibility over that of the prion strain. Simply put, the cells would mount the same autophagic response regardless of prion strain and its associated properties. Conversely, if there was a difference in responses of these cells to different strains, it would indicate that there is an intrinsic property of the strains itself that plays a larger role in how the cell responds. If this second scenario were true, it would further support work done by Jeffrey, Bartz, and co-workers that have shown cellular processing of misfolded PrP to be a critical factor in cell susceptibility and degradation/clearance[167-169].

Another intriguing direction is to look at the relationship amongst the rate of cellular replication, rate of clearance, and expression level of PrP^C in relation to susceptibility to infection. There is work showing that the rate of replication is more important in determining prion infectivity than the differentiated state of the cell(s)[180, 181]. In addition, in order to accumulate PrP^{Sc} and progress the disease, the rate of PrP^{Sc} formation must exceed the rate of clearance[182]. It has been well established that PrP^C is a necessary substrate for PrP^{Sc} conversion. Based on these three factors, we can predict that cells with a high replication rate, high rate of clearance, and low expression of PrP^C will be the least susceptible to prion infection and those with a low replication rate, low rate of clearance, and high expression of PrP^C will be the most susceptible. The question is which of the three factors has the largest effect on cell susceptibility.

Summary

A synopsis of the study can be found in **Table 1**. Briefly, we demonstrated that there are differences in both basal autophagosome formation and basal levels of PrP^C among L929, N2a, and CAD5 cells. However, our initial hypothesis that the basal level of autophagy would be a dominant factor in cell susceptibility to *de novo* prion infection ended up being wrong. In our experiments we found the opposite – cells with the highest levels of basal autophagy (L929) were far more susceptible to *de novo* prion infection compared to either CAD5 or N2a cells. In addition to this, the idea that expression levels of PrP^C would also factor into cell susceptibility was also found to be a non-factor, as L929 cells had a significantly lower level of PrP^C expression compared to N2a and CAD5 cells. This later point was supported by studies with fibroblasts, which showed that regardless of the expression levels of Mo3F4 PrP^{SEN} (PrP^C), cells accumulated comparable levels of PrP^{RES} (PrP^{Sc}) [94].

We hypothesised that augmenting autophagosome formation would increase resistance in cell susceptibility to prion infection and found this to be true. *De novo* infected L929 cells treated with trehalose resulted in an absence of PrP^{Sc} signal in late passages for all experiments compared to control *de novo* L929 infections, where over half had PrP^{Sc} signal return in late passages. In addition, we expanded on the results obtained by Aguib and colleagues [99], which showed that ongoing induction of autophagy by trehalose over time was able to clear infectious prion material from chronically infected ScN2a cells; we were able to show the same effect in chronically infected CAD5-RML cells.

The final aspect of our hypothesis was that inhibition of autophagy could make cells more susceptible to prion infection. We found that treatment with wortmannin rendered N2a and CAD5 cells slightly more susceptible to *de novo* prion infection than control *de novo* infections. We found that 1/6 and 4/9 experiments were positive for PrP^{Sc} signal in late passages in N2a and CAD5 cells, respectively, whereas both control N2a and CAD5 cell infections resulted in no return in PrP^{Sc} signal in late passages. *De Novo* infected L929 cells treated with wortmannin, however, had the opposite result of what we expected – none of the 9 experiments returned with PrP^{Sc} in late passages compared to over half of the control *de novo* infection experiments. When we analyzed the autophagosome formation rate, we discovered that on average there was no significant change, and in some cases, the rate increased. After some investigation we

determined that wortmannin had degraded due to its low stability in aqueous solutions at pH 3-8 (our culture media has a pH of 7.4). In spite of wortmannin degrading, we were able to see an increase in prion susceptibility in both neuronal cell lines, where 1/6 and 4/9 experiments were positive for PrP^{Sc} in late passages for N2a and CAD5 cells, respectively, compared to control *de novo* infections where none of the experiments were positive. Therefore, we can neither confirm nor deny our hypothesis that we could increase cell susceptibility by inhibiting autophagy. What we can say, however, is that in N2a and CAD5 cells, autophagosome formation rate in early passages, but not late passages, plays an important role in predicting whether PrP^{Sc} signal will return.

References

1. Safar, J. G. *et al*. Search for a prion-specific nucleic acid. *J. Virol.* **79**, 10796-10806 (2005).

2. Castilla, J., Saa, P., Hetz, C. & Soto, C. In vitro generation of infectious scrapie prions. *Cell* **121**, 195-206 (2005).

3. Deleault, N. R., Harris, B. T., Rees, J. R. & Supattapone, S. Formation of native prions from minimal components in vitro. *Proc. Natl. Acad. Sci. U. S. A.* **104**, 9741-9746 (2007).

4. Brandner, S. *et al*. Normal host prion protein (PrPC) is required for scrapie spread within the central nervous system. *Proc. Natl. Acad. Sci. U. S. A.* **93**, 13148-13151 (1996).

5. Smirnovas, V. *et al*. Structural organization of brain-derived mammalian prions examined by hydrogen-deuterium exchange. *Nat. Struct. Mol. Biol.* **18**, 504-506 (2011).

6. Collinge, J., Sidle, K. C., Meads, J., Ironside, J. & Hill, A. F. Molecular analysis of prion strain variation and the aetiology of 'new variant' CJD. *Nature* **383**, 685-690 (1996).

7. Aguzzi, A. & Polymenidou, M. Mammalian prion biology: one century of evolving concepts. *Cell* **116**, 313-327 (2004).

8. Martins, V. R. A receptor for infectious and cellular prion protein. *Braz. J. Med. Biol. Res.* **32**, 853-859 (1999).

9. Lee, K. S., Linden, R., Prado, M. A., Brentani, R. R. & Martins, V. R. Towards cellular receptors for prions. *Rev. Med. Virol.* **13**, 399-408 (2003).

10. Marc, D., Mercey, R. & Lantier, F. Scavenger, transducer, RNA chaperone? What ligands of the prion protein teach us about its function. *Cell Mol. Life Sci.* **64**, 815-829 (2007).

11. Linden, R. *et al*. Physiology of the prion protein. *Physiol. Rev.* **88**, 673-728 (2008).

12. Haas, L. T., Kostylev, M. A. & Strittmatter, S. M. Therapeutic molecules and endogenous ligands regulate the interaction between brain cellular prion protein (PrPC) and metabotropic glutamate receptor 5 (mGluR5). *J. Biol. Chem.* **289**, 28460-28477 (2014).

13. Isaacs, J. D., Jackson, G. S. & Altmann, D. M. The role of the cellular prion protein in the immune system. *Clin. Exp. Immunol.* **146**, 1-8 (2006).

14. Herms, J. *et al*. Evidence of presynaptic location and function of the prion protein. *J. Neurosci.* **19**, 8866-8875 (1999).

15. Haeberle, A. M. *et al*. Synaptic prion protein immuno-reactivity in the rodent cerebellum. *Microsc. Res. Tech.* **50**, 66-75 (2000).

16. D'Ambrosi, N. & Rossi, L. Copper at synapse: Release, binding and modulation of neurotransmission. *Neurochem. Int.* **90**, 36-45 (2015).

17. Brown, D. R. *et al*. The cellular prion protein binds copper in vivo. *Nature* **390**, 684-687 (2025).

18. Vassallo, N. & Herms, J. Cellular prion protein function in copper homeostasis and redox signalling at the synapse. *J. Neurochem.* **86**, 538-544 (2003).

19. Chiesa, R. The elusive role of the prion protein and the mechanism of toxicity in prion disease. *PLoS Pathog.* **11**, e1004745 (2015).

20. Portt, L., Norman, G., Clapp, C., Greenwood, M. & Greenwood, M. T. Anti-apoptosis and cell survival: a review. *Biochim. Biophys. Acta* **1813**, 238-259 (2011).

21. Schmitt-Ulms, G. *et al*. Time-controlled transcardiac perfusion cross-linking for the study of protein interactions in complex tissues. *Nat. Biotechnol.* **22**, 724-731 (2004).

22. Coitinho, A. S. *et al*. Decreased hyperlocomotion induced by MK-801, but not amphetamine and caffeine in mice lacking cellular prion protein (PrP(C)). *Brain Res. Mol. Brain Res.* **107**, 190-194 (2002).

23. Khosravani, H. *et al*. Prion protein attenuates excitotoxicity by inhibiting NMDA receptors. *J. Gen. Physiol.* **131**, i5 (2008).

24. Um, J. W. *et al*. Alzheimer amyloid-beta oligomer bound to postsynaptic prion protein activates Fyn to impair neurons. *Nat. Neurosci.* **15**, 1227-1235 (2012).

25. Zanata, S. M. *et al*. Stress-inducible protein 1 is a cell surface ligand for cellular prion that triggers neuroprotection. *EMBO J.* **21**, 3307-3316 (2002).

26. Coitinho, A. S. *et al*. The interaction between prion protein and laminin modulates memory consolidation. *Eur. J. Neurosci.* **24**, 3255-3264 (2006).

27. Kellett, K. A. & Hooper, N. M. Prion protein and Alzheimer disease. *Prion* **3**, 190-194 (2009).

28. Zhou, J. & Liu, B. Alzheimer's disease and prion protein. *Intractable Rare Dis. Res.* **2**, 35-44 (2013).

29. Nygaard, H. B. & Strittmatter, S. M. Cellular prion protein mediates the toxicity of beta-amyloid oligomers: implications for Alzheimer disease. *Arch. Neurol.* **66**, 1325-1328 (2009).

30. Basler, K. *et al*. Scrapie and cellular PrP isoforms are encoded by the same chromosomal gene. *Cell* **46**, 417-428 (1986).

31. Lee, I. Y. *et al*. Complete genomic sequence and analysis of the prion protein gene region from three mammalian species. *Genome Res.* **8**, 1022-1037 (1998).

32. Schatzl, H. M., Da Costa, M., Taylor, L., Cohen, F. E. & Prusiner, S. B. Prion protein gene variation among primates. *J. Mol. Biol.* **245**, 362-374 (1995).

33. Stahl, N., Borchelt, D. R., Hsiao, K. & Prusiner, S. B. Scrapie prion protein contains a phosphatidylinositol glycolipid. *Cell* **51**, 229-240 (1987).

34. Velayos, J. L. *et al*. Cellular prion protein in the central nervous system of mammals. Anatomoclinical associations. *Neurologia* **25**, 228-233 (2010).

35. Etlinger, J. D. & Goldberg, A. L. A soluble ATP-dependent proteolytic system responsible for the degradation of abnormal proteins in reticulocytes. *Proc. Natl. Acad. Sci. U. S. A.* **74**, 54-58 (1977).

36. Haas, A. L., Warms, J. V., Hershko, A. & Rose, I. A. Ubiquitin-activating enzyme. Mechanism and role in protein-ubiquitin conjugation. *J. Biol. Chem.* **257**, 2543-2548 (1982).

37. Lee, P. C., Sowa, M. E., Gygi, S. P. & Harper, J. W. Alternative ubiquitin activation/conjugation cascades interact with N-end rule ubiquitin ligases to control degradation of RGS proteins. *Mol. Cell* **43**, 392-405 (2011).

38. Aguzzi, A., Nuvolone, M. & Zhu, C. The immunobiology of prion diseases. *Nat. Rev. Immunol.* **13**, 888-902 (2013).

39. Houston, F., Foster, J. D., Chong, A., Hunter, N. & Bostock, C. J. Transmission of BSE by blood transfusion in sheep. *Lancet* **356**, 999-1000 (2000).

40. Hadlow, W. J., Race, R. E. & Kennedy, R. C. Temporal distribution of transmissible mink encephalopathy virus in mink inoculated subcutaneously. *J. Virol.* **61**, 3235-3240 (1987).

41. Sigurdson, C. J. *et al*. Oral transmission and early lymphoid tropism of chronic wasting disease PrPres in mule deer fawns (Odocoileus hemionus). *J. Gen. Virol.* **80 (Pt 10)**, 2757-2764 (1999).

42. Mohri, S., Handa, S. & Tateishi, J. Lack of effect of thymus and spleen on the incubation period of Creutzfeldt-Jakob disease in mice. *J. Gen. Virol.* **68 (Pt 4)**, 1187-1189 (1987).

43. Aguzzi, A., Heikenwalder, M. & Polymenidou, M. Insights into prion strains and neurotoxicity. *Nat. Rev. Mol. Cell Biol.* **8**, 552-561 (2007).

44. Fraser, H. & Dickinson, A. G. Scrapie in mice. Agent-strain differences in the distribution and intensity of grey matter vacuolation. *J. Comp. Pathol.* **83**, 29-40 (1973).

45. Bruce, M. E. & Fraser, H. Scrapie strain variation and its implications. *Curr. Top. Microbiol. Immunol.* **172**, 125-138 (1991).

46. Bessen, R. A. *et al*. Non-genetic propagation of strain-specific properties of scrapie prion protein. *Nature* **375**, 698-700 (1995).

47. Deleault, N. R., Lucassen, R. W. & Supattapone, S. RNA molecules stimulate prion protein conversion. *Nature* **425**, 717-720 (2003).

48. Ma, J. The role of cofactors in prion propagation and infectivity. *PLoS Pathog.* **8**, e1002589 (2012).

49. Mead, S. *et al*. Balancing selection at the prion protein gene consistent with prehistoric kurulike epidemics. *Science* **300**, 640-643 (2003).

50. Goldfarb, L. G. *et al*. Fatal familial insomnia and familial Creutzfeldt-Jakob disease: disease phenotype determined by a DNA polymorphism. *Science* **258**, 806-808 (1992).

51. Brown, K. & Mastrianni, J. A. The prion diseases. *J. Geriatr. Psychiatry Neurol.* **23**, 277-298 (2010).

52. Asante, E. A. *et al*. A naturally occurring variant of the human prion protein completely prevents prion disease. *Nature* **522**, 478-481 (2015).

53. Pattison, I. H. The relative susceptibility of sheep, goats and mice to two types of the goat scrapie agent. *Res. Vet. Sci.* **7**, 207-212 (1966).

54. Collinge, J. & Clarke, A. R. A general model of prion strains and their pathogenicity. *Science* **318**, 930-936 (2007).

55. Bessen, R. A. & Marsh, R. F. Distinct PrP properties suggest the molecular basis of strain variation in transmissible mink encephalopathy. *J. Virol.* **68**, 7859-7868 (1994).

56. Caughey, B., Raymond, G. J. & Bessen, R. A. Strain-dependent differences in beta-sheet conformations of abnormal prion protein. *J. Biol. Chem.* **273**, 32230-32235 (1998).

57. Piro, J. R., Harris, B. T. & Supattapone, S. In situ photodegradation of incorporated polyanion does not alter prion infectivity. *PLoS Pathog.* **7**, e1002001 (2011).

58. Gabizon, R., McKinley, M. P., Groth, D. F., Kenaga, L. & Prusiner, S. B. Properties of scrapie prion protein liposomes. *J. Biol. Chem.* **263**, 4950-4955 (1988).

59. Bell, J. E. & Ironside, J. W. Neuropathology of spongiform encephalopathies in humans. *Br. Med. Bull.* **49**, 738-777 (1993).

60. Wells, G. A., Wilesmith, J. W. & McGill, I. S. Bovine spongiform encephalopathy: a neuropathological perspective. *Brain Pathol.* **1**, 69-78 (1991).

61. Jeffrey, M. *et al.* Early unsuspected neuron and axon terminal loss in scrapie-infected mice revealed by morphometry and immunocytochemistry. *Neuropathol. Appl. Neurobiol.* **21**, 41-49 (1995).

62. Gains, M. J. & LeBlanc, A. C. Canadian Association of Neurosciences Review: prion protein and prion diseases: the good and the bad. *Can. J. Neurol. Sci.* **34**, 126-145 (2007).

63. Kim, Y. S., Carp, R. I., Callahan, S. M. & Wisniewski, H. M. Incubation periods and survival times for mice injected stereotaxically with three scrapie strains in different brain regions. *J. Gen. Virol.* **68 (Pt 3)**, 695-702 (1987).

64. Mackenzie, A. Immunohistochemical demonstration of glial fibrillary acidic protein in scrapie. *J. Comp. Pathol.* **93**, 251-259 (1983).

65. Jeffrey, M., Goodbrand, I. A. & Goodsir, C. M. Pathology of the transmissible spongiform encephalopathies with special emphasis on ultrastructure. *Micron* **26**, 277-298 (1995).

66. van der Merwe, J., Aiken, J., Westaway, D. & McKenzie, D. The standard scrapie cell assay: development, utility and prospects. *Viruses* **7**, 180-198 (2015).

67. Mahal, S. P. *et al.* Prion strain discrimination in cell culture: the cell panel assay. *Proc. Natl. Acad. Sci. U. S. A.* **104**, 20908-20913 (2007).

68. Li, J., Browning, S., Mahal, S. P., Oelschlegel, A. M. & Weissmann, C. Darwinian evolution of prions in cell culture. *Science* **327**, 869-872 (2010).

69. Oelschlegel, A. M. & Weissmann, C. Acquisition of drug resistance and dependence by prions. *PLoS Pathog.* **9**, e1003158 (2013).

70. Schweichel, J. U. & Merker, H. J. The morphology of various types of cell death in prenatal tissues. *Teratology* **7**, 253-266 (1973).

71. Liberski, P. P., Brown, D. R., Sikorska, B., Caughey, B. & Brown, P. Cell death and autophagy in prion diseases (transmissible spongiform encephalopathies). *Folia Neuropathol.* **46**, 1-25 (2008).

72. Liberski, P. P., Sikorska, B., Bratosiewicz-Wasik, J., Gajdusek, D. C. & Brown, P. Neuronal cell death in transmissible spongiform encephalopathies (prion diseases) revisited: from apoptosis to autophagy. *Int. J. Biochem. Cell Biol.* **36**, 2473-2490 (2004).

73. Melino, G., Knight, R. A. & Nicotera, P. How many ways to die? How many different models of cell death? *Cell Death Differ.* **12 Suppl 2**, 1457-1462 (2005).

74. Roucou, X. & LeBlanc, A. C. Cellular prion protein neuroprotective function: implications in prion diseases. *J. Mol. Med. (Berl)* **83**, 3-11 (2005).

75. Soto, C. & Satani, N. The intricate mechanisms of neurodegeneration in prion diseases. *Trends Mol. Med.* **17**, 14-24 (2011).

76. Kurschner, C. & Morgan, J. I. Analysis of interaction sites in homo- and heteromeric complexes containing Bcl-2 family members and the cellular prion protein. *Brain Res. Mol. Brain Res.* **37**, 249-258 (1996).

77. Mouillet-Richard, S. *et al*. Signal transduction through prion protein. *Science* **289**, 1925-1928 (2000).

78. Prinz, M. *et al*. Intrinsic resistance of oligodendrocytes to prion infection. *J. Neurosci.* **24**, 5974-5981 (2004).

79. Chesebro, B. *et al*. Anchorless prion protein results in infectious amyloid disease without clinical scrapie. *Science* **308**, 1435-1439 (2005).

80. Migheli, A., Attanasio, A., Lee, W. H., Bayer, S. A. & Ghetti, B. Detection of apoptosis in weaver cerebellum by electron microscopic in situ end-labeling of fragmented DNA. *Neurosci. Lett.* **199**, 53-56 (1995).

81. Engelstein, R., Grigoriadis, N., Greig, N. H., Ovadia, H. & Gabizon, R. Inhibition of P53-related apoptosis had no effect on PrP(Sc) accumulation and prion disease incubation time. *Neurobiol. Dis.* **18**, 282-285 (2005).

82. Christensen, H. M. *et al*. A highly toxic cellular prion protein induces a novel, nonapoptotic form of neuronal death. *Am. J. Pathol.* **176**, 2695-2706 (2010).

83. Jamieson, E., Jeffrey, M., Ironside, J. W. & Fraser, J. R. Apoptosis and dendritic dysfunction precede prion protein accumulation in 87V scrapie. *Neuroreport* **12**, 2147-2153 (2001).

84. Heiseke, A., Aguib, Y. & Schatzl, H. M. Autophagy, prion infection and their mutual interactions. *Curr. Issues Mol. Biol.* **12**, 87-97 (2010).

85. Ragagnin, A., Guillemain, A., Grant, N. J. & Bailly, Y. J. R. in *Autophagy - A Double Edged Sword - Cell Survival or Death* (ed Bailly, Y. J. R.) (InTech.

86. Shin, H. Y., Oh, J. M. & Kim, Y. S. The Functional Role of Prion Protein (PrPC) on Autophagy. *Pathogens* **2**, 436-445 (2013).

87. Yao, H., Zhao, D., Khan, S. H. & Yang, L. Role of autophagy in prion protein-induced neurodegenerative diseases. *Acta Biochim. Biophys. Sin. (Shanghai)* **45**, 494-502 (2013).

88. Goold, R., McKinnon, C. & Tabrizi, S. J. Prion degradation pathways: Potential for therapeutic intervention. *Mol. Cell. Neurosci.* **66**, 12-20 (2015).

89. Renna, M., Jimenez-Sanchez, M., Sarkar, S. & Rubinsztein, D. C. Chemical inducers of autophagy that enhance the clearance of mutant proteins in neurodegenerative diseases. *J. Biol. Chem.* **285**, 11061-11067 (2010).

90. Ishibashi, D. *et al*. Strain-Dependent Effect of Macroautophagy on Abnormally Folded Prion Protein Degradation in Infected Neuronal Cells. *PLoS One* **10**, e0137958 (2015).

91. Smith, P. K. *et al*. Measurement of protein using bicinchoninic acid. *Anal. Biochem.* **150**, 76-85 (1985).

92. Powers, J. C., Asgian, J. L., Ekici, O. D. & James, K. E. Irreversible inhibitors of serine, cysteine, and threonine proteases. *Chem. Rev.* **102**, 4639-4750 (2002).

93. Kimura, S., Fujita, N., Noda, T. & Yoshimori, T. Monitoring autophagy in mammalian cultured cells through the dynamics of LC3. *Methods Enzymol.* **452**, 1-12 (2009).

94. Vorberg, I., Raines, A., Story, B. & Priola, S. A. Susceptibility of common fibroblast cell lines to transmissible spongiform encephalopathy agents. *J. Infect. Dis.* **189**, 431-439 (2004).

95. Yamaguchi, S. *et al*. Inhibition of PrPSc formation by synthetic O-sulfated glycopyranosides and their polymers. *Biochem. Biophys. Res. Commun.* **349**, 485-491 (2006).

96. Prusiner, S. B. Novel proteinaceous infectious particles cause scrapie. *Science* **216**, 136-144 (1982).

97. Bueler, H. *et al*. Mice devoid of PrP are resistant to scrapie. *Cell* **73**, 1339-1347 (1993).

98. Sarkar, S., Davies, J. E., Huang, Z., Tunnacliffe, A. & Rubinsztein, D. C. Trehalose, a novel mTOR-independent autophagy enhancer, accelerates the clearance of mutant huntingtin and alpha-synuclein. *J. Biol. Chem.* **282**, 5641-5652 (2007).

99. Aguib, Y. *et al*. Autophagy induction by trehalose counteracts cellular prion infection. *Autophagy* **5**, 361-369 (2009).

100. Yang, Y. P. *et al*. Application and interpretation of current autophagy inhibitors and activators. *Acta Pharmacol. Sin.* **34**, 625-635 (2013).

101. Rubinsztein, D. C., Marino, G. & Kroemer, G. Autophagy and aging. *Cell* **146**, 682-695 (2011).

102. Ghavami, S. *et al*. Autophagy and apoptosis dysfunction in neurodegenerative disorders. *Prog. Neurobiol.* **112**, 24-49 (2014).

103. Stumpf, M. P. & Krakauer, D. C. Mapping the parameters of prion-induced neuropathology. *Proc. Natl. Acad. Sci. U. S. A.* **97**, 10573-10577 (2000).

104. Korolchuk, V. I., Menzies, F. M. & Rubinsztein, D. C. Mechanisms of cross-talk between the ubiquitin-proteasome and autophagy-lysosome systems. *FEBS Lett.* **584**, 1393-1398 (2010).

105. Kroemer, G., Marino, G. & Levine, B. Autophagy and the integrated stress response. *Mol. Cell* **40**, 280-293 (2010).

106. Kabeya, Y. *et al*. LC3, a mammalian homologue of yeast Apg8p, is localized in autophagosome membranes after processing. *EMBO J.* **19**, 5720-5728 (2000).

107. Sarkar, S. Regulation of autophagy by mTOR-dependent and mTOR-independent pathways: autophagy dysfunction in neurodegenerative diseases and therapeutic application of autophagy enhancers. *Biochem. Soc. Trans.* **41**, 1103-1130 (2013).

108. Mizushima, N., Yoshimori, T. & Levine, B. Methods in mammalian autophagy research. *Cell* **140**, 313-326 (2010).

109. Kang, R., Zeh, H. J., Lotze, M. T. & Tang, D. The Beclin 1 network regulates autophagy and apoptosis. *Cell Death Differ.* **18**, 571-580 (2011).

110. Hakkinen, K. M., Harunaga, J. S., Doyle, A. D. & Yamada, K. M. Direct comparisons of the morphology, migration, cell adhesions, and actin cytoskeleton of fibroblasts in four different three-dimensional extracellular matrices. *Tissue Eng. Part A.* **17**, 713-724 (2011).

111. Qi, Y., Wang, J. K., McMillian, M. & Chikaraishi, D. M. Characterization of a CNS cell line, CAD, in which morphological differentiation is initiated by serum deprivation. *J. Neurosci.* **17**, 1217-1225 (1997).

112. Veith, N. M., Plattner, H., Stuermer, C. A., Schulz-Schaeffer, W. J. & Burkle, A. Immunolocalisation of PrPSc in scrapie-infected N2a mouse neuroblastoma cells by light and electron microscopy. *Eur. J. Cell Biol.* **88**, 45-63 (2009).

113. Marijanovic, Z., Caputo, A., Campana, V. & Zurzolo, C. Identification of an intracellular site of prion conversion. *PLoS Pathog.* **5**, e1000426 (2009).

114. Beranger, F., Mange, A., Goud, B. & Lehmann, S. Stimulation of PrP(C) retrograde transport toward the endoplasmic reticulum increases accumulation of PrP(Sc) in prion-infected cells. *J. Biol. Chem.* **277**, 38972-38977 (2002).

115. Wang, J. & Maldonado, M. A. The ubiquitin-proteasome system and its role in inflammatory and autoimmune diseases. *Cell. Mol. Immunol.* **3**, 255-261 (2006).

116. Chen, B., Retzlaff, M., Roos, T. & Frydman, J. Cellular strategies of protein quality control. *Cold Spring Harb Perspect. Biol.* **3**, a004374 (2011).

117. Scotter, E. L. *et al*. Differential roles of the ubiquitin proteasome system and autophagy in the clearance of soluble and aggregated TDP-43 species. *J. Cell. Sci.* **127**, 1263-1278 (2014).

118. Kristiansen, M. *et al*. Disease-associated prion protein oligomers inhibit the 26S proteasome. *Mol. Cell* **26**, 175-188 (2007).

119. Andre, R. & Tabrizi, S. J. Misfolded PrP and a novel mechanism of proteasome inhibition. *Prion* **6**, 32-36 (2012).

120. Pandey, U. B. *et al*. HDAC6 rescues neurodegeneration and provides an essential link between autophagy and the UPS. *Nature* **447**, 859-863 (2007).

121. Marzo, L. *et al*. 4-hydroxytamoxifen leads to PrPSc clearance by conveying both PrPC and PrPSc to lysosomes independently of autophagy. *J. Cell. Sci.* **126**, 1345-1354 (2013).

122. McKinnon, C. *et al*. Prion-mediated neurodegeneration is associated with early impairment of the ubiquitin-proteasome system. *Acta Neuropathol.* **131**, 411-425 (2016).

123. Bian, J. *et al*. Cell-based quantification of chronic wasting disease prions. *J. Virol.* **84**, 8322-8326 (2010).

124. Courageot, M. P. *et al*. A cell line infectible by prion strains from different species. *J. Gen. Virol.* **89**, 341-347 (2008).

125. Kim, H. J. *et al*. Establishment of a cell line persistently infected with chronic wasting disease prions. *J. Vet. Med. Sci.* **74**, 1377-1380 (2012).

126. Ladogana, A., Liu, Q., Xi, Y. G. & Pocchiari, M. Proteinase-resistant protein in human neuroblastoma cells infected with brain material from Creutzfeldt-Jakob patient. *Lancet* **345**, 594-595 (1995).

127. Raymond, G. J. *et al*. Inhibition of protease-resistant prion protein formation in a transformed deer cell line infected with chronic wasting disease. *J. Virol.* **80**, 596-604 (2006).

128. Ghaemmaghami, S. *et al*. Cell division modulates prion accumulation in cultured cells. *Proc. Natl. Acad. Sci. U. S. A.* **104**, 17971-17976 (2007).

129. Grassmann, A., Wolf, H., Hofmann, J., Graham, J. & Vorberg, I. Cellular aspects of prion replication in vitro. *Viruses* **5**, 374-405 (2013).

130. Weissmann, C. The state of the prion. *Nat. Rev. Microbiol.* **2**, 861-871 (2004).

131. Bosque, P. J. & Prusiner, S. B. Cultured cell sublines highly susceptible to prion infection. *J. Virol.* **74**, 4377-4386 (2000).

132. Chasseigneaux, S. *et al*. Genetic heterogeneity versus molecular analysis of prion susceptibility in neuroblasma N2a sublines. *Arch. Virol.* **153**, 1693-1702 (2008).

133. Race, R. The scrapie agent in vitro. *Curr. Top. Microbiol. Immunol.* **172**, 181-193 (1991).

134. Race, R. E., Fadness, L. H. & Chesebro, B. Characterization of scrapie infection in mouse neuroblastoma cells. *J. Gen. Virol.* **68 (Pt 5)**, 1391-1399 (1987).

135. Butler, D. A. *et al*. Scrapie-infected murine neuroblastoma cells produce protease-resistant prion proteins. *J. Virol.* **62**, 1558-1564 (1988).

136. Solassol, J., Crozet, C. & Lehmann, S. Prion propagation in cultured cells. *Br. Med. Bull.* **66**, 87-97 (2003).

137. Caughey, B. & Raymond, G. J. Sulfated polyanion inhibition of scrapie-associated PrP accumulation in cultured cells. *J. Virol.* **67**, 643-650 (1993).

138. Birkett, C. R. *et al*. Scrapie strains maintain biological phenotypes on propagation in a cell line in culture. *EMBO J.* **20**, 3351-3358 (2001).

139. Yun, S. W. *et al*. The tyrosine kinase inhibitor imatinib mesylate delays prion neuroinvasion by inhibiting prion propagation in the periphery. *J. Neurovirol.* **13**, 328-337 (2007).

140. Heiseke, A., Aguib, Y., Riemer, C., Baier, M. & Schatzl, H. M. Lithium induces clearance of protease resistant prion protein in prion-infected cells by induction of autophagy. *J. Neurochem.* **109**, 25-34 (2009).

141. Cortes, C. J., Qin, K., Cook, J., Solanki, A. & Mastrianni, J. A. Rapamycin delays disease onset and prevents PrP plaque deposition in a mouse model of Gerstmann-Straussler-Scheinker disease. *J. Neurosci.* **32**, 12396-12405 (2012).

142. Benjamin, D., Colombi, M., Moroni, C. & Hall, M. N. Rapamycin passes the torch: a new generation of mTOR inhibitors. *Nat. Rev. Drug Discov.* **10**, 868-880 (2011).

143. Mitra, S., Tsvetkov, A. S. & Finkbeiner, S. Protein turnover and inclusion body formation. *Autophagy* **5**, 1037-1038 (2009).

144. Mardones, P., Rubinsztein, D. C. & Hetz, C. Mystery solved: Trehalose kickstarts autophagy by blocking glucose transport. *Sci. Signal.* **9**, fs2 (2016).

145. DeBosch, B. J. *et al*. Trehalose inhibits solute carrier 2A (SLC2A) proteins to induce autophagy and prevent hepatic steatosis. *Sci. Signal.* **9**, ra21 (2016).

146. Beranger, F., Crozet, C., Goldsborough, A. & Lehmann, S. Trehalose impairs aggregation of PrPSc molecules and protects prion-infected cells against oxidative damage. *Biochem. Biophys. Res. Commun.* **374**, 44-48 (2008).

147. Singer, M. A. & Lindquist, S. Multiple effects of trehalose on protein folding in vitro and in vivo. *Mol. Cell* **1**, 639-648 (1998).

148. Gilles, R., Bourdouxhe-Housiaux, C., Colson, P. & Houssier, C. Effect of compensatory organic osmolytes on resistance to freeze-drying of L929 cells and of their isolated chromatin. *Comp. Biochem. Physiol. A. Mol. Integr. Physiol.* **122**, 145-155 (1999).

149. Mussauer, H., Sukhorukov, V. L. & Zimmermann, U. Trehalose improves survival of electrotransfected mammalian cells. *Cytometry* **45**, 161-169 (2001).

150. Mizushima, N. & Levine, B. Autophagy in mammalian development and differentiation. *Nat. Cell Biol.* **12**, 823-830 (2010).

151. Tsukamoto, S. *et al*. Autophagy is essential for preimplantation development of mouse embryos. *Science* **321**, 117-120 (2008).

152. Hara, T. *et al*. Suppression of basal autophagy in neural cells causes neurodegenerative disease in mice. *Nature* **441**, 885-889 (2006).

153. Seglen, P. O. & Gordon, P. B. 3-Methyladenine: specific inhibitor of autophagic/lysosomal protein degradation in isolated rat hepatocytes. *Proc. Natl. Acad. Sci. U. S. A.* **79**, 1889-1892 (1982).

154. Wu, Y. T. *et al*. Dual role of 3-methyladenine in modulation of autophagy via different temporal patterns of inhibition on class I and III phosphoinositide 3-kinase. *J. Biol. Chem.* **285**, 10850-10861 (2010).

155. McNamara, C. R. & Degterev, A. Small-molecule inhibitors of the PI3K signaling network. *Future Med. Chem.* **3**, 549-565 (2011).

156. Hou, H. *et al*. Inhibitors of phosphatidylinositol 3'-kinases promote mitotic cell death in HeLa cells. *PLoS One* **7**, e35665 (2012).

157. Keyse & Stephen, M. (2000)Stress Response - Methods and Protocols .

158. EFSA Scientific Committee. Statistical Significance and Biological Relevance. *EFSA Journal* **9**, n/a (2011).

159. Kovacs, G. G. *et al*. Mutations of the prion protein gene phenotypic spectrum. *J. Neurol.* **249**, 1567-1582 (2002).

160. Klohn, P. C., Stoltze, L., Flechsig, E., Enari, M. & Weissmann, C. A quantitative, highly sensitive cell-based infectivity assay for mouse scrapie prions. *Proc. Natl. Acad. Sci. U. S. A.* **100**, 11666-11671 (2003).

161. Marbiah, M. M. *et al*. Identification of a gene regulatory network associated with prion replication. *EMBO J.* **33**, 1527-1547 (2014).

162. Imberdis, T. & Harris, D. A. Prion permissive pathways: extracellular matrix genes control susceptibility to prion infection. *EMBO J.* **33**, 1506-1508 (2014).

163. DebBurman, S. K., Raymond, G. J., Caughey, B. & Lindquist, S. Chaperone-supervised conversion of prion protein to its protease-resistant form. *Proc. Natl. Acad. Sci. U. S. A.* **94**, 13938-13943 (1997).

164. Deleault, N. R. *et al*. Protease-resistant prion protein amplification reconstituted with partially purified substrates and synthetic polyanions. *J. Biol. Chem.* **280**, 26873-26879 (2005).

165. Abid, K., Morales, R. & Soto, C. Cellular factors implicated in prion replication. *FEBS Lett.* **584**, 2409-2414 (2010).

166. Derrington, E. *et al*. PrPC has nucleic acid chaperoning properties similar to the nucleocapsid protein of HIV-1. *C. R. Biol.* **325**, 17-23 (2002).

167. Jeffrey, M., McGovern, G., Goodsir, C. M., Siso, S. & Gonzalez, L. Strain-associated variations in abnormal PrP trafficking of sheep scrapie. *Brain Pathol.* **19**, 1-11 (2009).

168. Gonzalez, L., Martin, S. & Jeffrey, M. Distinct profiles of PrP(d) immunoreactivity in the brain of scrapie- and BSE-infected sheep: implications for differential cell targeting and PrP processing. *J. Gen. Virol.* **84**, 1339-1350 (2003).

169. Ayers, J. I. *et al*. The strain-encoded relationship between PrP replication, stability and processing in neurons is predictive of the incubation period of disease. *PLoS Pathog.* **7**, e1001317 (2011).

170. Dall'Armi, C., Devereaux, K. A. & Di Paolo, G. The role of lipids in the control of autophagy. *Curr. Biol.* **23**, 33 (2013).

171. Shatz, O., Holland, P., Elazar, Z. & Simonsen, A. Complex Relations Between Phospholipids, Autophagy, and Neutral Lipids. *Trends Biochem. Sci.* **41**, 907-923 (2016).

172. Poluzzi, C. *et al*. Endorepellin evokes autophagy in endothelial cells. *J. Biol. Chem.* **289**, 16114-16128 (2014).

173. Neill, T., Schaefer, L. & Iozzo, R. V. Instructive roles of extracellular matrix on autophagy. *Am. J. Pathol.* **184**, 2146-2153 (2014).

174. Viegas, P. *et al*. Junctional expression of the prion protein PrPC by brain endothelial cells: a role in trans-endothelial migration of human monocytes. *J. Cell. Sci.* **119**, 4634-4643 (2006).

175. Simak, J., Holada, K., D'Agnillo, F., Janota, J. & Vostal, J. G. Cellular prion protein is expressed on endothelial cells and is released during apoptosis on membrane microparticles found in human plasma. *Transfusion* **42**, 334-342 (2002).

176. Shikiya, R. A. *et al*. PrPSc formation and clearance as determinants of prion tropism. *PLoS Pathog.* **13**, e1006298 (2017).

177. Vella, L. J. *et al*. Packaging of prions into exosomes is associated with a novel pathway of PrP processing. *J. Pathol.* **211**, 582-590 (2007).

178. Guo, B. B., Bellingham, S. A. & Hill, A. F. Stimulating the Release of Exosomes Increases the Intercellular Transfer of Prions. *J. Biol. Chem.* **291**, 5128-5137 (2016).

179. Abduhrahman, B. A., Abdelaziz, D. H., Nishikawa, S. & Schatzl, H. Autophagy Controls Exosomal Release of Prions and Lateral Prion Infection. *The FASEB Journal* **30**, Suppl. 1062.1 (2016).

180. Herbst, A. *et al*. Infectious prions accumulate to high levels in non proliferative C2C12 myotubes. *PLoS Pathog.* **9**, e1003755 (2013).

181. Herbst, A., Aiken, J. M. & McKenzie, D. Replication of prions in differentiated muscle cells. *Prion* **8**, 27890. Epub 2014 Feb 11 (2014).

182. Aguzzi, A. & Zhu, C. Five questions on prion diseases. *PLoS Pathog.* **8**, e1002651 (2012).